NAVAL POSTGRADUATE SCHOOL

MONTEREY, CALIFORNIA

THESIS

DESIGN AND DEVELOPMENT OF A COUNTER-SWARM PROTOTYPE AIR VEHICLE

by

Kai Grohe

December 2017

Thesis Advisor:	Christopher Brophy
Second Reader:	Oleg Yakimenko

THIS PAGE INTENTIONALLY LEFT BLANK

REPORT DOCUMENTATION PAGE			Form Approved OMB No. 0704–0188
Public reporting burden for this collection of information is estimated to average 1 hour per response, including the time for reviewing instruction, searching existing data sources, gathering and maintaining the data needed, and completing and reviewing the collection of information. Send comments regarding this burden estimate or any other aspect of this collection of information, including suggestions for reducing this burden, to Washington headquarters Services, Directorate for Information Operations and Reports, 1215 Jefferson Davis Highway, Suite 1204, Arlington, VA 22202-4302, and to the Office of Management and Budget, Paperwork Reduction Project (0704-0188) Washington, DC 20503.			
1. AGENCY USE ONLY ***(Leave blank)***	**2. REPORT DATE** December 2017	**3. REPORT TYPE AND DATES COVERED** Master's thesis	
4. TITLE AND SUBTITLE DESIGN AND DEVELOPMENT OF A COUNTER-SWARM PROTOTYPE AIR VEHICLE		**5. FUNDING NUMBERS**	
6. AUTHOR(S) Kai Grohe			
7. PERFORMING ORGANIZATION NAME(S) AND ADDRESS(ES) Naval Postgraduate School Monterey, CA 93943-5000		**8. PERFORMING ORGANIZATION REPORT NUMBER**	
9. SPONSORING /MONITORING AGENCY NAME(S) AND ADDRESS(ES) N/A		**10. SPONSORING / MONITORING AGENCY REPORT NUMBER**	
11. SUPPLEMENTARY NOTES The views expressed in this thesis are those of the author and do not reflect the official policy or position of the Department of Defense or the U.S. Government. IRB number N/A.			
12a. DISTRIBUTION / AVAILABILITY STATEMENT Approved for public release. Distribution is unlimited.		**12b. DISTRIBUTION CODE**	

13. ABSTRACT (maximum 200 words)

Small weaponized unmanned aerial vehicles (UAV) that leverage new commercially available technologies are an emerging low-cost and easily available threat. These inexpensive vehicles can threaten ground forces and warships and easily overwhelm air defenses through saturation attacks, which are cost-effective due to the low unit cost. Current air defense systems are designed to counter low quantities of very capable but extremely expensive weapons, and in many cases cannot properly defend against attacks involving a large number of offensive weapons. To avoid the scenario of an opponent overmatching current defenses with emerging low-cost weapons, a missile-based interceptor system is proposed. This vehicle also makes use of new low-cost, high-performance commercial-off-the shelf (COTS) technology to attain the required performance metrics and deliver a payload capable of defeating multiple units, while still remaining cost-effective against the threat of low-cost small UAVs. This thesis describes the development of the mission, aerodynamic, structural, and recovery systems of a prototype vehicle intended to show that the concept of a low-cost delivery system for a counter UAV payload is valid and worthy of further development. Completion of such a vehicle covers a gap in existing air defense systems, disallowing adversaries an opportunity for tactical advantage.

14. SUBJECT TERMS counter UAV, UAV defeat, low-cost missile, missile design			**15. NUMBER OF PAGES** 119
			16. PRICE CODE
17. SECURITY CLASSIFICATION OF REPORT Unclassified	**18. SECURITY CLASSIFICATION OF THIS PAGE** Unclassified	**19. SECURITY CLASSIFICATION OF ABSTRACT** Unclassified	**20. LIMITATION OF ABSTRACT** UU

THIS PAGE INTENTIONALLY LEFT BLANK

Approved for public release. Distribution is unlimited.

DESIGN AND DEVELOPMENT OF A COUNTER-SWARM PROTOTYPE AIR VEHICLE

Kai Grohe
Captain, Royal Canadian Air Force
BME, Concordia University, 2011

Submitted in partial fulfillment of
the requirements for the degrees of

MASTER OF SCIENCE IN MECHANICAL ENGINEERING

and

MASTER OF SCIENCE IN ENGINEERING SCIENCE
(AEROSPACE ENGINEERING)

from the

NAVAL POSTGRADUATE SCHOOL
December 2017

Approved by: Christopher Brophy
Thesis Advisor

Oleg Yakimenko
Second Reader

Garth V. Hobson
Chair, Department of Mechanical and Aerospace Engineering

THIS PAGE INTENTIONALLY LEFT BLANK

ABSTRACT

Small weaponized unmanned aerial vehicles (UAV) that leverage new commercially available technologies are an emerging low-cost and easily available threat. These inexpensive vehicles can threaten ground forces and warships and easily overwhelm air defenses through saturation attacks, which are cost-effective due to the low unit cost. Current air defense systems are designed to counter low quantities of very capable but extremely expensive weapons, and in many cases cannot properly defend against attacks involving a large number of offensive weapons. To avoid the scenario of an opponent overmatching current defenses with emerging low-cost weapons, a missile-based interceptor system is proposed. This vehicle also makes use of new low-cost, high-performance commercial-off-the shelf (COTS) technology to attain the required performance metrics and deliver a payload capable of defeating multiple units, while still remaining cost-effective against the threat of low-cost small UAVs. This thesis describes the development of the mission, aerodynamic, structural, and recovery systems of a prototype vehicle intended to show that the concept of a low-cost delivery system for a counter UAV payload is valid and worthy of further development. Completion of such a vehicle covers a gap in existing air defense systems, disallowing adversaries an opportunity for tactical advantage.

THIS PAGE INTENTIONALLY LEFT BLANK

TABLE OF CONTENTS

LIST OF FIGURES

LIST OF TABLES

THIS PAGE INTENTIONALLY LEFT BLANK

LIST OF ACRONYMS AND ABBREVIATIONS

C	Celsius
CG	Center of gravity
CN	Coefficient of normal force
CP	Center of pressure
COTS	Commercial off the shelf
CRUSER	Consortium for robotics and unmanned systems education and research
DATCOM	Data compendium
DC	Direct current
deg	Degree
GNC	Guidance navigation and control
in	Inch
INS	Inertial navigation system
lbs	Pounds
m	Meter
mi	Miles
mm	Millimeter
MBT	Main battle tank
NPS	Naval Postgraduate School
oz	Ounce
ROS	Robot operating system
SUAVE	Small unmanned aerial vehicle eliminator
TVC	Thrust vector control
UAV	Unmanned aerial vehicle

THIS PAGE INTENTIONALLY LEFT BLANK

ACKNOWLEDGMENTS

I would like to thank Dr. Chris Brophy for providing me the opportunity to perform this work at the Rocket Lab and for his continuous support, guidance, and enthusiasm throughout the project.

Thank you to all the ME4704 students who lent a hand (willingly or otherwise) toward advancing this project. LT Busta and RCAF CAPT Lobo deserve thanks for getting engaged and dirtying their hands. LT Wagner requires thanks for needlessly suffering the desert heat in support of firing rockets. Thank you to the NPS Rocket Lab staff of Andrew Chaves, Lee van Houtte, and Dave Dausen for their constant work in making the rocket fly, and Robert Wright deserves a special thanks for his engagement in and passion for the minutiae of rocket and machine design. Detail work is a regular occurrence in engineering work, but it is those people who are keen and excited when they either investigate or beat down those details (as required) who make the work really worthwhile.

Last and most importantly, thank you to my family and friends, especially Anya and Inga. Your support and encouragement are special to me.

THIS PAGE INTENTIONALLY LEFT BLANK

I. INTRODUCTION

A. OVERVIEW

Based on the continuing decrease in cost of computing power of microprocessors and electronic controllers [1], [2] in the form of electronic servo controls and guidance technologies, an emerging threat to the forces of established nation states may be weaponized low-cost unmanned aerial vehicles (UAV) [3]. These low-cost weapon systems offer low to modest kinematic performance, but could be produced for a very small fraction of the cost of traditional weapon systems, thereby constituting a serious threat due to the relative quantity of these moderately capable enemy systems. This specific concept is exemplified by a 2017 incident, wherein a Patriot missile was used to engage a low-cost UAV. The issue this brings to light is summed in the following quote by Justin Bronk of the Royal United Services Institute:

> exposes in very stark terms the challenge which militaries face in attempting to deal with the adaptation of cheap and readily available civilian technology with extremely expensive, high-end hardware designed for state-on-state warfare. [4]

Such systems are being developed by many states and organizations [5], [6], [7], [8]. Efforts to develop a counter to these systems are being actively pursued [9], but to date the author is unaware of any systems having been adopted. This is largely due to the difficulty in effectively defeating a low-cost UAV [10]. Due to the nature of their size and construction, these vehicles are very survivable. A defeat method therefore currently requires the use of over-capable expensive weapons, and so the defensive cost using existing technology is much higher than the offensive cost.

An example of the threat with which this thesis is concerned is a weaponized version of the Naval Postgraduate School (NPS) consortium for robotics and unmanned systems education and research (CRUSER) swarm UAV

as seen in Figure 1. Such a vehicle has a wingspan of approximately 1.5 m (59.1 in), and a (unarmed) unit cost of approximately $300 [11].

Figure 1. Example of Low-Cost UAVs. Source: [12].

Low-cost UAVs can offer value as both strategic and tactical weapons. By creating a threat sufficient to demand defensive action on the part of the defender, these weapons can achieve several effects, partly dependent on the manner in which the defender reacts (for example: withdrawal, active or passive defenses, or attempting to ignore the threat). If a defender actively defends, then they are committing resources to this defense which could be used elsewhere. If the committed resources are high cost munitions from a limited stockpile, then the defender risks exhausting their stockpile, or incurring significantly higher costs than the attacker. When a defender expends greater resources in defense

than an attacker in offense, this is a strategic loss for the defender. From a tactical view, low-cost UAVs can be fitted with explosives/warheads which can inflict significant personnel or materiel damage and are therefore relevant weapons which must be addressed.

B. MOTIVATION

Due to the particularly low cost of the weaponized UAVs being considered, it is especially important to scale the cost of the defensive system relative to the cost of the threat [4]. Existing counters, such as surface to air intercept missiles cost from $38k for a FIM-92 Stinger [13] missile, to $3M for a PAC-3 Patriot [14] missile. Failure to scale the defensive expenditure to the offensive expenditure can result in depleting stockpiles of more capable defensive weapons, thereby degrading the defensive potential of an existing defensive system, or otherwise defeating the defender by forcing them to consume their own resources more rapidly than the adversary. This use was pioneered by the Israelis in the 1973 Yom Kippur War [15].

In order to avoid becoming vulnerable to the threat of low-cost UAVs [4], a defensive system with costs comparable to the system against which it is to defend, is important. One such system could leverage commercial off the shelf (COTS) components in a manner similar to the low-cost UAV threat. By using COTS rocket motors and controllers such as small form factor processors and sensors, the system can have a long storage life and a unit cost low enough to negate the system cost advantage of a small UAV.

C. OBJECTIVES AND APPROACH

> The existing [stovepipe] processes of research, definition of the requirement, technological development and acquisition are no longer up to date, neither is their inertia. Under resource constraints and time constraints the most viable solutions are the most flexible ones, those which combine capabilities in systems of systems. [16]

In accordance with the intent espoused in [16]'s quote, a vehicle referred to as the Small Unmanned Aerial Vehicle Eliminator (abbreviated as SUAVE) is

being studied as a counter to the threat of small, low-cost UAVs. The intent of this system is to leverage and marry emerging high-tech, low-cost technology with existing low-cost systems that provide sufficient performance to meet the minimum mission requirements, such that the resulting system offers a minimum cost solution to the problem. In so doing, the hope is to avoid the paradigm of stovepipe solutions, and offer a system that allows configuration and employment flexibility through accessible software and a low unit cost. Additionally, such a system could also be updated to take advantage of technology improvements through a modular design architecture.

To meet the low-cost target, it was decided that the detection, tracking, and targeting systems would be located off-board the flight vehicle and would communicate with the flight vehicle via data link. It is conceived that a missile-based payload delivery system can deliver a payload which can neutralize multiple low-cost UAV threats, thereby keeping the defensive expenditure roughly equivalent to the offensive expenditure. Systems required to complete the SUAVE as an implementable weapon system other than the flight vehicle were deemed outside the scope of this thesis.

Such a defensive system requires design and development efforts to prove the concept to be cost effective relative to the threat. This thesis covers early design and development work in the direction of proving that the concept can meet the performance requirements, in terms of kinematics and cost. The objectives of this thesis are further narrowed to focus on the following.

- Definition of the threat
- SUAVE mission plan
- Establishing a performance baseline
- Aerodynamic development

The approach pursues the creation of a flight vehicle, intended to provide desired performance characteristics for evaluation and validation against

performance predictions. This flight vehicle is intended to be a platform for continued development, and is therefore designed with recovery systems in place of a destructive payload.

Additional aspects of the SUAVE development program that took place during the period that the author worked on the SUAVE are covered as well. It is hoped that this will ease future SUAVE work by consolidating important information.

THIS PAGE INTENTIONALLY LEFT BLANK

II. BACKGROUND

A. REVIEW OF THREAT

The assumed threat is a small (approx. 1 to 1.5 m [39.4 to 59.1 in] wingspan) low-cost weaponized UAV employed as a munition, which consists of high and low tech systems, such that the various components required by the air vehicle are all low-cost components. The small UAV considered is a fixed-wing vehicle intended to leverage technology developed for the hobbyist small aircraft market. This vehicle is described in some literature as a drone, but is not to be confused with a rotary wing aircraft, which relies on propeller thrust continuously directed toward the ground to maintain an altitude. Vehicles relying on constant vertical thrust are not considered within the range of threats with which this thesis is concerned, as rotary winged aircraft of this sort are a much easier target due to their increased complexity and reliance on constant thrust production to remain airborne. It is believed that if the SUAVE can defeat fixed wing UAVs, then it will readily defeat rotary wing UAVs. Review to verify the SUAVE's capability against rotary wing UAVs is recommended for future work.

The vehicle considered would be similar to the AeroVironment Switchblade [17]. The Switchblade functions in a very similar manner, but offers increased portability and data-linking technology at a related unit cost (~$70k/ unit) [18]. The higher unit cost alters some of the employment economics, and the proposed small UAV is meant to gain advantage from the low-cost potential of this technology. This type of vehicle has benefited greatly in recent years from the commercial introduction of high-energy density batteries, small and affordable powerful digitally controlled brushless motors, and low-cost micro-controllers and computers. These components, when mated to an airframe of some variety of expanded plastic, create a very affordable air vehicle which displays some potentially useful performance specifications. Due to the particularly low system cost, these vehicles are less like traditional aircraft (which are generally too expensive to be disposable), and more like munitions (such as

rockets or artillery projectiles). Due to the small size of the system, logistic concerns are greatly relieved. The equipment can be easily transported in any existing utility truck, and does not require multi-ton infrastructure such as that required to deliver artillery projectiles (ie. The artillery piece itself). The entire system is envisioned to consist of a general purpose transport truck fitted with a launch catapult (such as that employed by the NPS CRUSER group), storage for the small UAVs themselves, and an electronic control center offering communications and data links in order to process fire mission requests and upload target coordinates into the small UAVs control sets. This system (transport truck and disposable small UAV munitions) can then be employed in a variety of roles. Based on an initial, non-optimized review of COTS components, the proposed system offers the capability to deliver individual payloads of approximately 2 kg (4.41 lbs) (similar to a RPG-7 warhead, or a 60mm (2.36 in) mortar) at ranges equivalent to 155mm (6.1 in) howitzers. The vehicles can accept GPS signals for guidance, or rely on an internal IMU when operating in a GPS denied environment. A 2 kg (4.41 lbs) Shaped Charge Jet with a fragmenting case threatens both armour and personnel, allowing a target set of anything less armoured than a main battle tank or bunker.

This type of small UAV is an indiscriminate weapon, and not expected to see service amongst organized nations governed by rule of law and carrying a concern for international military law, specifically related to minimizing civilian casualties. This style of small UAV would be employed in an offensive role, targeting locations by flying to pre-programmed coordinate sets, or employing sufficiently low-cost on-board sensors. They are not expected to have data links in order to avoid associated susceptibilities to EW, and are therefore not provided oversight from ground controllers, and are not fitted with equipment for surveillance purposes.

1. Threat Concept of Operations

A target location is uploaded into the small UAV(s). A single (or more likely multiple) small UAV(s) are launched from the small UAV forward deployment vehicle (likely a transport truck fitted with a launch rail and storage racks for small UAVs). These vehicles will employ their own onboard guidance to navigate to the target location, in the same manner as Tomahawk missiles, detonating their payloads at the target location. The payload is assumed to consist of a lightweight warhead, potentially a shaped charge with a fragmenting external liner. This would allow a small UAV to cause significant and relevant damage to armoured targets, as well as minor damage to other equipment and personnel casualties from non-direct hits. As these weapons would be capable of inflicting damage to an adversary, a method of defense is required. Ideally the small UAV would be deemed sufficiently threatening to warrant a response, and so the defender will expend weapons stores, reducing their IADS potential against other more costly forms of airpower (helicopter gunships, close air support, etc.).

2. Threat as Air Defense Suppression

IADS are currently the most effective air defense technology. These systems are comprised of several separate weapons systems, each one itself being a capable air defense weapon system on its own. By integrating several weapon systems of varying capability, it is more difficult for an opponent to overwhelm the defender, because the IADS can perform target categorization and allocation, and distributed sensor networks provide synergy. Distributed and linked sensor networks present multiple directions from which a sensor may detect a target. Availability of multiple types of weapons provides several weapon options, from which the most advantageous can be selected. These features make an IADS difficult to defeat with the weapons it is intended to defend against.

Small UAVs offer several advantages when used for air defense system suppression. The low cost allows many small UAVs to be deployed against a

single anti-air battery, which can overwhelm the tracking and targeting systems of the defender. Because of the low cost, a high loss rate of small UAVs is entirely acceptable. This price difference allows the small UAVs to be used to cause the opponent to expend their weapon stocks in the same manner as the IDF caused Syrian forces to expend their air defense missiles in the 1973 Yom Kippur war [15]. Unlike the 1973 example, the small UAV threat will include an explosive, and is therefore not exclusively a decoy, as it cannot be ignored without repercussion. This forces the defender to respond to the small UAV threat. The defender is therefore forced into the position of expending expensive weapons to defeat the small UAVs [4], or losing assets from successful small UAV strikes. The defense therefore suffers tactical defeat from expending weapons stocks or losing assets, or suffers strategic defeat because the cost of defense is grossly larger than the cost of the offensive action [4].

3. Threat Performance Metrics

Analytic based performance predictions performed by the author in collaboration with RSAF Maj. Y. K. Qiu and RCAF Capt. K. Lobo indicate the following likely capabilities of the small UAV threat in Table 1:

Table 1. Threat Performance Metrics

Performance Metric	**Predicted Value**
Velocity	23.3 m/s (76.4 ft/s)
Payload	1.9 kg (4.19 lbs)
Endurance	20 mins
Estimated Cost	< $1000 / unit

B. DEFEAT CONCEPTS

Based on research [10], [19], [20], the defeat of a small UAV is a non-trivial task. The casual assumption regarding defeat mechanism is a soldier with a rifle or shotgun. Due to the particulars of a small UAV, this is not effective. Survivability is defined as the combination of susceptibility and vulnerability [21].

A small UAV has both low susceptibility and vulnerability. Susceptibility is “the inability of an aircraft to avoid being hit by one or more damage mechanisms in the pursuit of its mission” [21]. Small size decreases the ease of detection to a variety of detection, such as optical and radar, similar to how detection by human sight is decreased. To hit a target, it must first be seen [22]. Additionally, the materials from which many small UAVs are constructed reduce RCS [19]. The small electric motors used generate very little heat and therefore do not provide a large signal for infrared detectors. Vehicle sound is also quite low, which complicates audible detection. Once detected and fired upon, a small UAV is a small target, and therefore more difficult to hit than a large target, further increasing survivability.

Assuming the vehicle is detected in time for the defenders to respond, a small UAV’s vulnerability is also low. Vulnerability is defined as “the inability of the aircraft to withstand the damage caused by the man-made hostile environment” [21]. The UAV threat considered is comprised of only a few critical systems and components affixed to an airframe often made of an expanded plastic, often Expanded PolyOlefin (EPO) [23]. This construction design differs significantly from that of a traditional aircraft, which combines a highly stressed internal structure which carries the loads due to the weight and aerodynamic forces defined by the flight profile. A traditional construction becomes significantly degraded in terms of its ability to continue to bear flight loads once physically damaged from its original shape. Traditional aircraft are filled with large amounts of important equipment, and include large fuel containers that are especially vulnerable to penetration which can initiate fires. This means that a projectile striking the aircraft has a good chance of doing damage to an important component or system. A small UAV of expanded plastic has few or no highly stressed portions and instead often distributes structural loads evenly through the entire structure. This means that removal of a small portion of the structure does not appreciably increase associated stresses in the surviving structure, and the vehicles can therefore often continue to fly after being hit by projectiles. A

projectile hitting a small UAV has a good chance of passing through the target without damaging important components. The result is that a small UAV is relatively less vulnerable than a traditional aircraft. With low susceptibility and low vulnerability, a small UAV is very survivable in a man-made threat environment.

The question of how to defeat once detected is a complicated one. Options include the rifleman, armed with a small arm that fires solid small diameter projectiles or a large number of small diameter (2 – 9.7 mm (.08in - .38in)) [24] spheres (aka a shotgun). The odds of a successful ballistic hit can be improved in several ways. Increasing the number of projectiles fired at the threat increases the odds of a hit, but may be limited to what can be achieved with hand-held weapons. Mounting the weapon to something large can mitigate this. Automatic controls can provide increases in accuracy, but significantly increase the cost and complexity of the defensive system. A trade-off analysis between accuracy, system complexity, munition cost, and defeat effectiveness may show that rapid-fired, intelligently fused exploding projectiles may offer an excellent balance of overall cost and ultimate effectiveness. Further research into this topic is recommended. This thesis focuses on a system wherein the guidance and control functions have been built into the projectile (the missile), and the launcher itself includes no guidance or control systems.

Directed energy weapons are another option. Existing directed energy weapons suffer several issues with range, portability, operational limitations, and power requirements. As these weapons are being rapidly developed, many of these issues may soon be solved. However, directed energy weapons such as lasers would still need to cause physical damage to a small UAV; against which small UAVs are similarly resistant as against projectiles. Lasers also tend to heat a small area, which could melt or ignite the expanded plastic of a UAV. Perhaps future lasers will be able to slice through an expanded plastic airframe, but at this time no such system is known by the author to exist.

Directed energy weapons exist which can induce electric currents in targeted electronics, such as radar and similar systems. Solid state electronics

are susceptible to induced currents from electromagnetic waves [25]. A high-energy transmitter could be employed to project sufficient energy to seriously damage electronics. This type of weapon cannot be carefully directed, lending it an indiscriminate quality which makes it of questionable utility for a defensive application, where friendly forces will also likely be in the path of the same electromagnetic projection.

The lethality of a fragmenting munition can be tailored in terms of direction and distance from point of detonation. Fragment size and number of fragments for a given munition can be matched to overall weight for a certain effect via the Gurney Equation [26]. Determining the ideal size of fragment and CEP to achieve a UAV kill requires complicated analysis which almost inevitably involves experimentation [27]. A fragmenting munition can be sent as a projectile with a gun or missile to a location, which provides some measure of control over what collateral damage may be incurred. Fragmenting munitions tend to be heavy, which increases the cost of each munition, and the system as a whole. The fragment spray pattern can be tailored, allowing either more control over the affected area, or allowing the possibility of affecting multiple targets with a single munition. An analysis to determine the optimum warhead size for the small UAV threat as a function of multiple target dispersion distances and compared to the resulting warhead cost is recommended.

Assuming that a small UAV is constructed of a composite and/or expanded plastic airframe, the vehicle would be susceptible to heat and fire. A method of reliably applying heat or fire at distances of several hundred meters has not been determined. One possibility is a payload which would be dispersed over a target area before being ignited.

A small UAV's vulnerability to a given defeat mechanism is based on the physical interaction between that mechanism and the specific UAV component (such as the airframe or motor) in question. To properly catalogue the effectiveness of a particular defeat mechanism, a long sequence of analysis and experimentation is required [27]. Each component must be evaluated to

determine the interactions of any particular defeat mechanism of interest. The sum of a given defeat mechanism's effects across all the effected components determines the expected effectiveness of any given mechanism. Defeat mechanism effectiveness is outside the scope of this thesis, and so the vehicle is being designed to allow payload flexibility to support future selection and refinement of the defeat mechanism.

It is expected that based on the warhead effectiveness studies, cost effectiveness in terms of number of targets defeated compared to missile cost can be maximized by employing multiple submunitions. By using the SUAVE as a delivery mechanism similar to the CBU-97 [28], multiple targets can be engaged by a single defensive missile. Concepts of implementing this idea must be developed.

C. INTERCEPT SCENARIO

An assumed scenario for this system helps to illustrate the expected employment of the system being developed. This scenario is a land-based employment, but could occur at sea just as easily. The generic scenario is intended to familiarize the reader with the proposed concept such that the derivation of the metrics used during design have context.

A platoon (four vehicles) of Blue Team main battle tanks (MBT) has moved to occupy a forward position in a terrain of rolling hills and tree copses covering a stretch of road. Red Team scouts have spotted the MBTs and relayed the MBTs position to their command. This information is sent to the small UAV's launcher and transformed by automated computer program into navigation information by the UAV once the target location is loaded into the UAV. A flight of 30 UAVs are launched toward the MBTs at a unit cost of $1000 each, for a total attack cost of $30k. The flight plan is set such that the UAVs travel around several intervening hills so as to approach the target from an angle that allows an easy flight path into the targets. Using a catapult system, the UAVs are launched quickly from the transport vehicle so that a closed spaced line of UAVs are

headed en-route to the target. The UAVs are programmed to fly low, just over the treetops towards the target area. This low flight altitude further complicates the engagement for the defender, as it helps shield the UAVs from detection.

Blue Team is assumed to have intelligence indicating a potential attack by small UAVs, and therefore a dedicated small UAV detection system is included as an accessory on a support vehicle attached to the platoon. The detection system performance estimates are based on existing systems, which offer an advertised detection range of 1 km (0.621 mi) [29]. The automated detection system finds the incoming UAVs and begins processing. A firing solution is calculated by the targeting computers, and the SUAVE's arming lights begin illuminating as the vehicle automatically runs through pre-flight checks. In a short time, the SUAVE's motor ignites, and the vehicle is propelled straight up and out of its launch cylinder. With a careful motion of the aerodynamic control surfaces, the SUAVE begins a tight arc through the air as the vehicle positions itself to deploy the defeat payload against the incoming UAVs. The smooth arcing turn brings the SUAVE to a point above the flight of UAVs, where the payload is deployed and subsequently neutralizes the small UAVs. Blue Team's human elements are able to continue to carry out their primary jobs throughout the UAV / SUAVE engagement and focus on mission completion as near to uninterrupted as possible.

In another scenario, the SUAVE launcher is located somewhere within a networked battlespace. A remote detector confirms an incoming flight of small UAVs and sends their location to the SUAVE. The firing computer determines that the threat UAVs are just within range of the SUAVE system and commands launch. Aiming for a distant intercept, the firing solution is a semi-ballistic trajectory, which takes the SUAVE high into the air. Even after motor burnout, the SUAVE continues to control its orientation and trajectory. High efficiency aerodynamic design allows the SUAVE to cover large amounts of distance with its relatively small rocket motor. The SUAVE then drifts down upon the enemy, to where it can optimally release its payload and defeat the opponents.

D. SUAVE CONCEPT OF OPERATIONS

In analyzing the scenario in Chapter II. Sec. C. Intercept Scenario to determine performance targets for the system, the short range case is used to set the primary goals, because the short range kinematics are more important for the missile's goal of providing a defense against a close range threat. If a SUAVE is deployed in a forward defensive role, it must be able to defeat an incoming threat which has just been detected. Failure to complete the short range intercept means that the SUAVE is unable to defend its own location, and limits the employment of the SUAVE. A desired goal of the SUAVE system is to provide an automatic defensive capability to forward deployed units. The SUAVE should be installed as a defensive accessory which does not require additional attention to activate. This keeps the forward elements free to act and removes the potential of small UAVs to effectively harass an opponent. Therefore, the SUAVE should be able to intercept and defeat incoming small UAVs in a distance related to the intercept distance.

As a defensive accessory to existing vehicles, it is desired that the SUAVE launch from a vertical position and maneuver to intercept. To aim the SUAVE, the launch system becomes large; for example, the current Phalanx close in weapon system weighs 6200 kg (13668.6 lbs) [30]. This weight includes a large number of unguided projectiles, while the SUAVE system will rely on a few guided projectiles which keeps the launcher from being saddled with aiming functions and thus the weight down. By launching from a vertical position, the SUAVE is capable of the same performance in 360 degrees from the launch location. An automated detection system is to be included, which will calculate and transmit target location information to the SUAVE. The SUAVE will carry out its own guidance, navigation, and control (GNC) functions by relating the provided target location to its own self-measured position. Using a solid fuel rocket motor for propulsion, the SUAVE can be kept in a ready-to-launch condition, and the entire sequence automated. Since from target detection to

SUAVE launch no human operator is required, the humans will suffer minimal distraction from enemy attack and remain focused on their tasks.

Intercepts can be categorized as either short or long range. A short range intercept occurs when the SUAVE is collocated with the small UAV's target; this is discussed in more detail in Chapter II. Sec. F. Short Range Intercept. In the long range case, a SUAVE launcher is not collocated with the small UAV target, is networked into the battlespace, or is otherwise able to be fed target location information, and is within effective range of the expected intercept location. In this case, the SUAVE is required to perform some amount of maneuvering to arrive at a distant location. The driving question for the long-range intercept is the effective range of the SUAVE. Effective range is dependent on the exact flight profile and energy management, which itself is a function of the control algorithm. Maximizing the range can be achieved by control optimization and refinement of the aerodynamic layout required to meet the short range intercept requirements. Since short range capability allows the vehicle to protect and be transported by front-line combat groups, no additional organization is required to provide a SUAVE-based shield. Therefore, the short-range intercept is chosen as being the primary design target.

E. DESIGN PROCESS

The intent of this thesis is to research and further develop this concept which began as a project of NPS's ME4704 Missile Design course. While the ME4704 course has investigated several different elements, this thesis focused on aerodynamic development to create a recoverable and functional air vehicle for test and evaluation uses. The vehicle is reusable, and will allow empirical investigation of exact aerodynamic properties which are difficult to predict with existing software [31].

A design process specific to tactical missile design, seen in Figure 2, was used as a development guide for this effort and can be found in [32]. This

process provides an approach founded on practical experience and emphasizes the intent of a missile, which is to accomplish a very specific task.

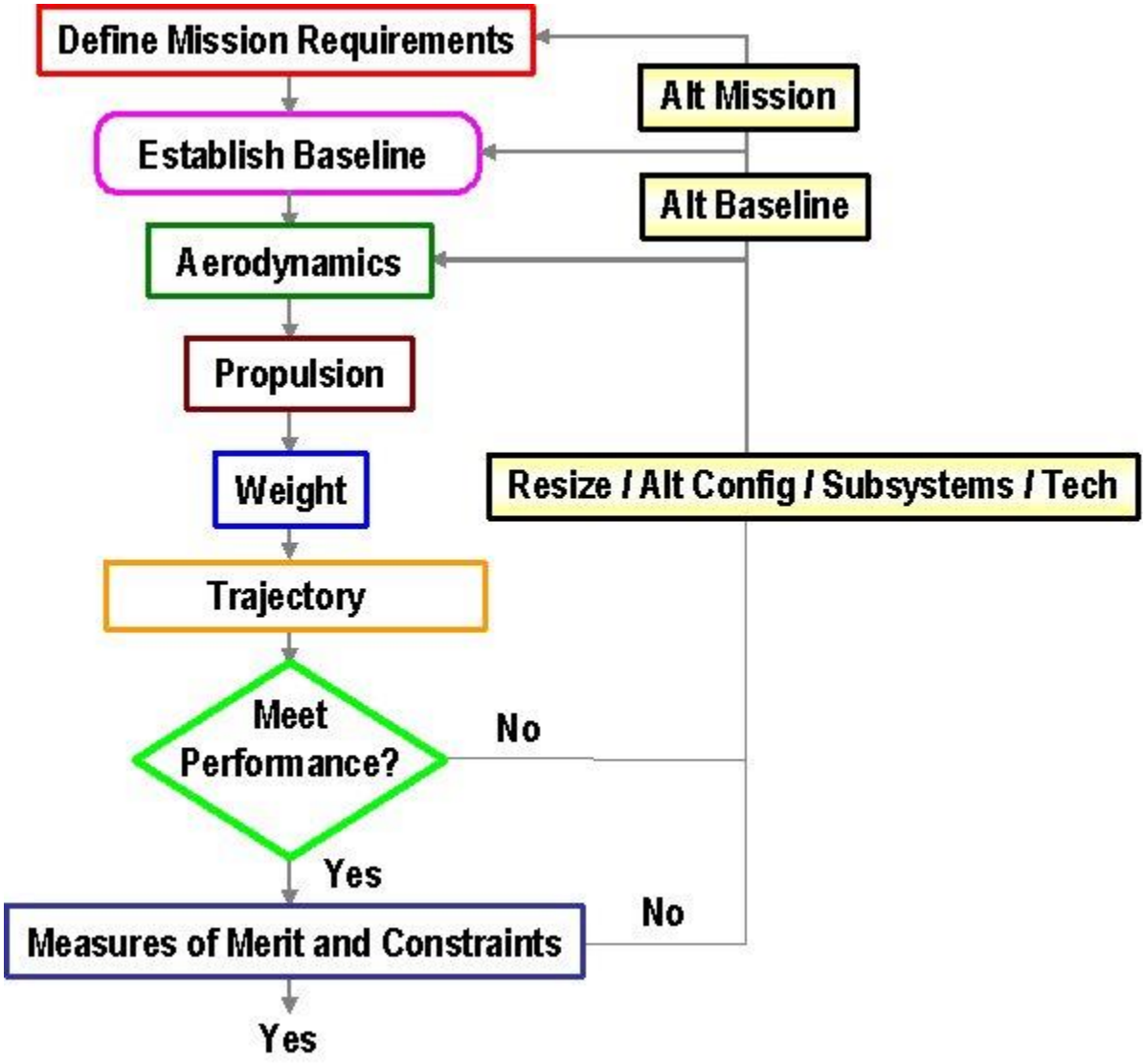

Figure 2. Fleeman's Missile Design Process. Source: [32].

Unsurprisingly, the first step as presented by Fleeman is therefore an analysis of what the vehicle needs to do in terms of kinematics and payload. After the performance requirements have been established, the design is pursued by assembling solutions to each of the subsystems which comprise a

missile. The complete assembly of design solutions can then be reviewed as appropriate to gauge the performance that the system as a whole should provide. This predicted performance is then compared against the performance requirements. If the performance requirements are met, then the design can proceed either to further refinement as required (especially in the case of review of conceptual designs) or alteration for manufacture vice prototype in the case of more advanced designs. An interesting aspect of Fleeman's missile design process is that it includes a decision step where if a design does not meet performance requirements, then alteration of either the mission or baseline performance is suggested. This can be compared to a generic design process presented in Figure 3.

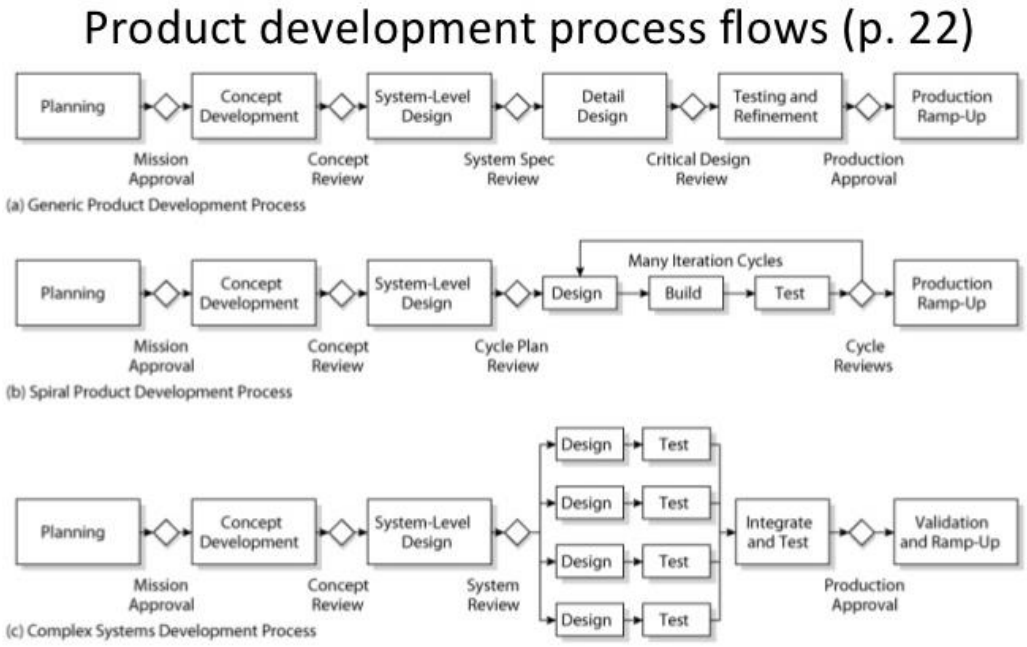

Figure 3. Generic Product Design Process. Source: [33].

The generic design process does not include Fleeman's first step. It is unknown if this due to the expense involved in bringing a missile design to a given level of development, or simply to the comparison between a generic design process and one tailored to a specific product. Since a flight vehicle is a

system of systems, the generic design process can be applied to any of a missile's subsystems, and was used a guideline through this thesis work.

Design of a missile is a relatively complex engineering activity, involving many engineering specialties. A missile requires some form of propulsion and a comprehensive knowledge of available propulsion systems provided by the propulsion engineer to achieve the desired thrust profile and velocity. Once airborne, it is the aerodynamic forces prescribed by the aerodynamicist that determine the missile's orientation and often the majority of the flight characteristics. After the fuel has been consumed, aerodynamic forces alone provide the dynamics that govern the vehicle's kinematics. A missile must have sufficient structure so as to ensure that all geometric relations between systems, components, or parts of components, remain within acceptable limits throughout the intended flight profile, generally known as the structural rigidity. High rigidity must be balanced with the increases of weight that generally come with increasing rigidity, which is the job of the structural engineer. A guidance system and seeker, if so equipped, and most control systems will require complex electronics, most often itself controlled through software. The seeker and electronics are the domain of the electrical engineer, while the controller will be a collaborative effort of a combination of software, computer, electrical, or other engineering specialties. Each of these systems that comprise a missile are interrelated to varying degrees, so that successful design requires managing the various specialist's resource requirements. Fleeman provides an illustrative cartoon regarding this aspect as competition within aerospace as systems engineering in Figure 4.

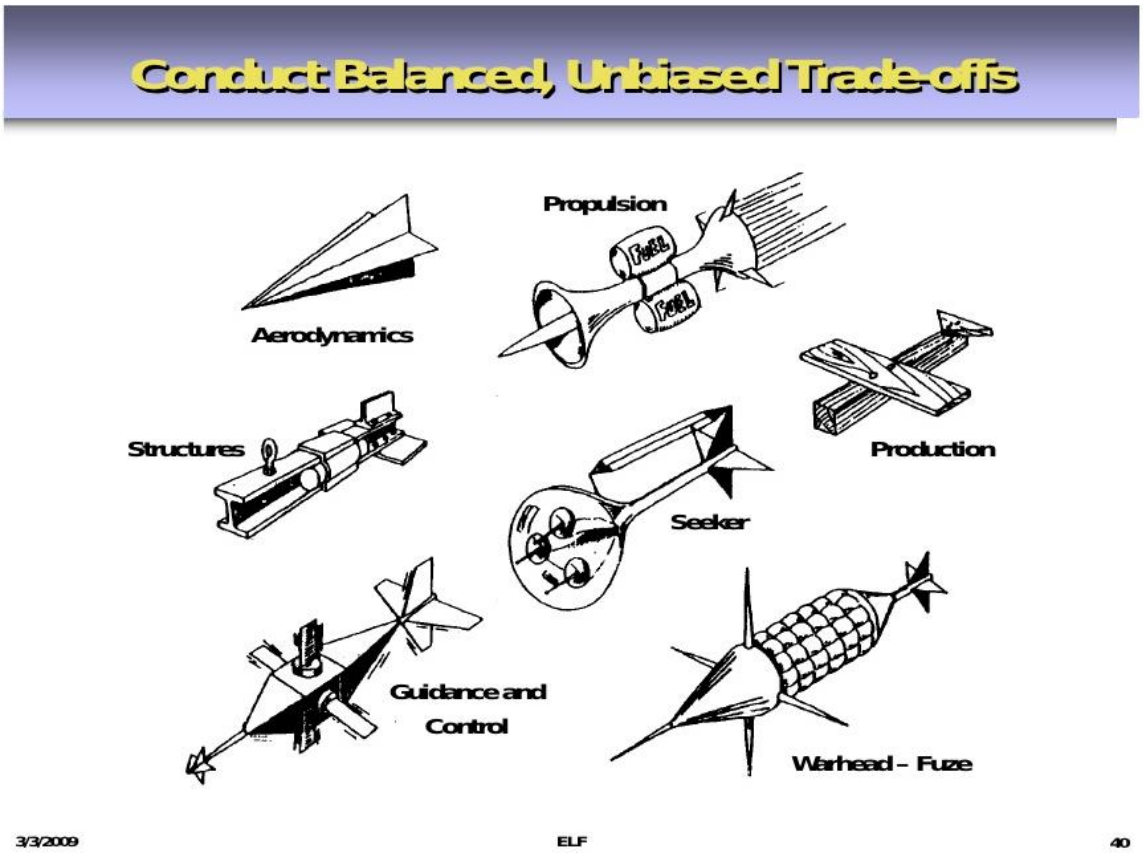

Figure 4. Design of a System Requires Balancing System Needs.
Source: [32].

A design process flow is recommended by Fleeman and shown in Figure 5. This process provides a relatively clear path forward for missile design efforts. It should be noted that this path is not sequential, as various specialist output must be fed into analysis used to guide the decision-making of other specialists. This is represented by the parallel activities which feed common activity blocks in the diagram.

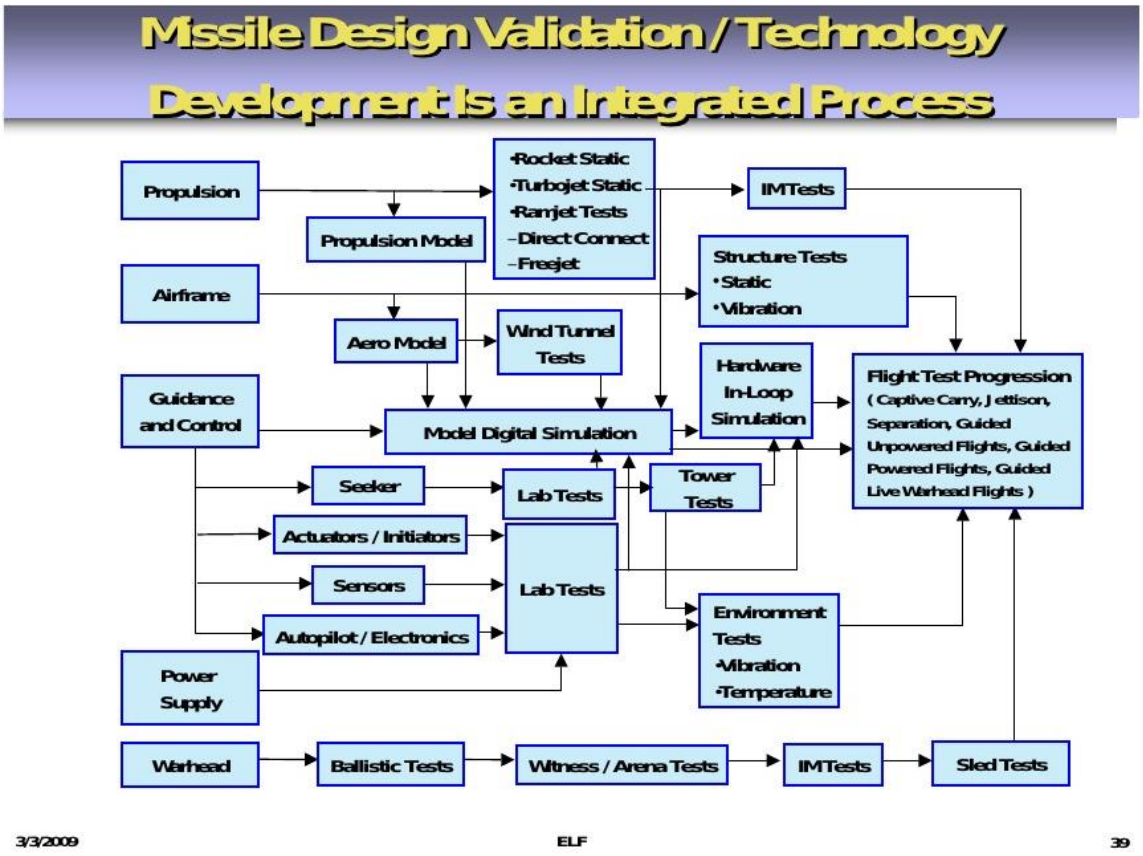

Figure 5. Most-Clear Path to Missile Design. Source: [32].

It should be noted that while Fleeman's recommended process provides a relatively clear path, this specific thesis' design effort came to rely on a path dependency not shown in the diagram but added in Figure 6. Specifically the control surface actuator selection drove aerodynamic design due to actuator limitations tied to size and component cost.

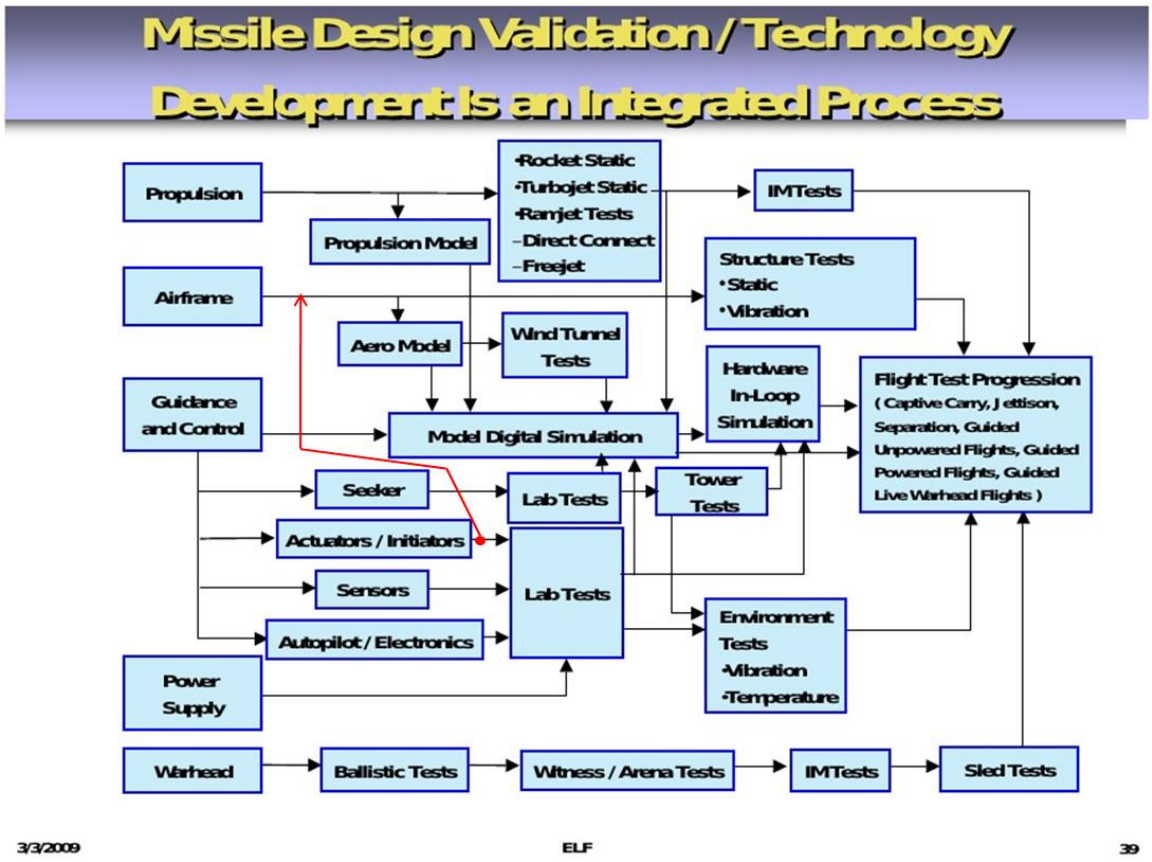

Figure 6. Specific Case Requirements of a General Process.
Source: [32].

It is not believed that this exception to Fleeman's general design process in any way invalidates it; rather, it is believed that the minor addition of a signal connection shows how well the process captures the activities and flow involved in missile design. Fleeman's process provides a good generalized flow to design activities. It does not serve as a Gantt chart, as it provides no clues regarding the amount of effort, hours, or resources required for each identified activity.

The scope of activities required to bring a missile from concept to production is quite large. Most of the individual activities are themselves quite complex. It is for these reasons that the SUAVE design is best approached as a program vice project, where a program is defined as a collection of projects

which each contribute toward a common goal. Each individual project has defined deliverables which are expected to match the time and resources allocated to that project. This particular thesis therefore explores one design project within the larger SUAVE program.

It should be noted that this report includes the most recent values obtained throughout the design process. It is not a detailed record of the values used at different stages of the design which may have since been superseded by more accurate values. The values reported are intended to reflect the current state of development and allow the program to be further progressed.

F. SHORT RANGE INTERCEPT

When the UAVs are headed directly toward a target with a collocated SUAVE, the SUAVE is required to rapidly turn from its initial vertical heading and maneuver to the optimal location to deploy its payload. This is described as the short-range intercept case. In terms of kinematic requirements, the short-range intercept is the most challenging, as it requires significant amounts of force directed to the center of the turn. This force will come from both the vehicle's aerodynamics, and partly from the rocket thrust by carefully balancing the vehicle at an angle relative to its forward motion. This short-range intercept creates a challenging flight condition for the vehicle to adopt. As mentioned earlier, ability to achieve a short range intercept allows the SUAVE to be integrated as an automated defense system carried by forward elements, with little to no additional considerations in order to ensure their effectiveness.

1. Rationale for Aerodynamic Control

With the intent to create a flight vehicle capable of its own guidance and control, some method(s) of affecting the vehicle's orientation must be included. There are several options for achieving missile orientation control. For missile flight, control of the vehicle's orientation with respect to both the inertial reference (conveniently chosen as the earth's surface for most tactical applications) and the angle of the airflow over the body are important. The vehicle orientation with

regards to something else is described as being in relation to a reference frame; here we discuss the inertial reference frame and the wind frame. Figure 7 is a diagram of the angle and force naming convention used by Missile DATCOM and adopted for use in this project [34].

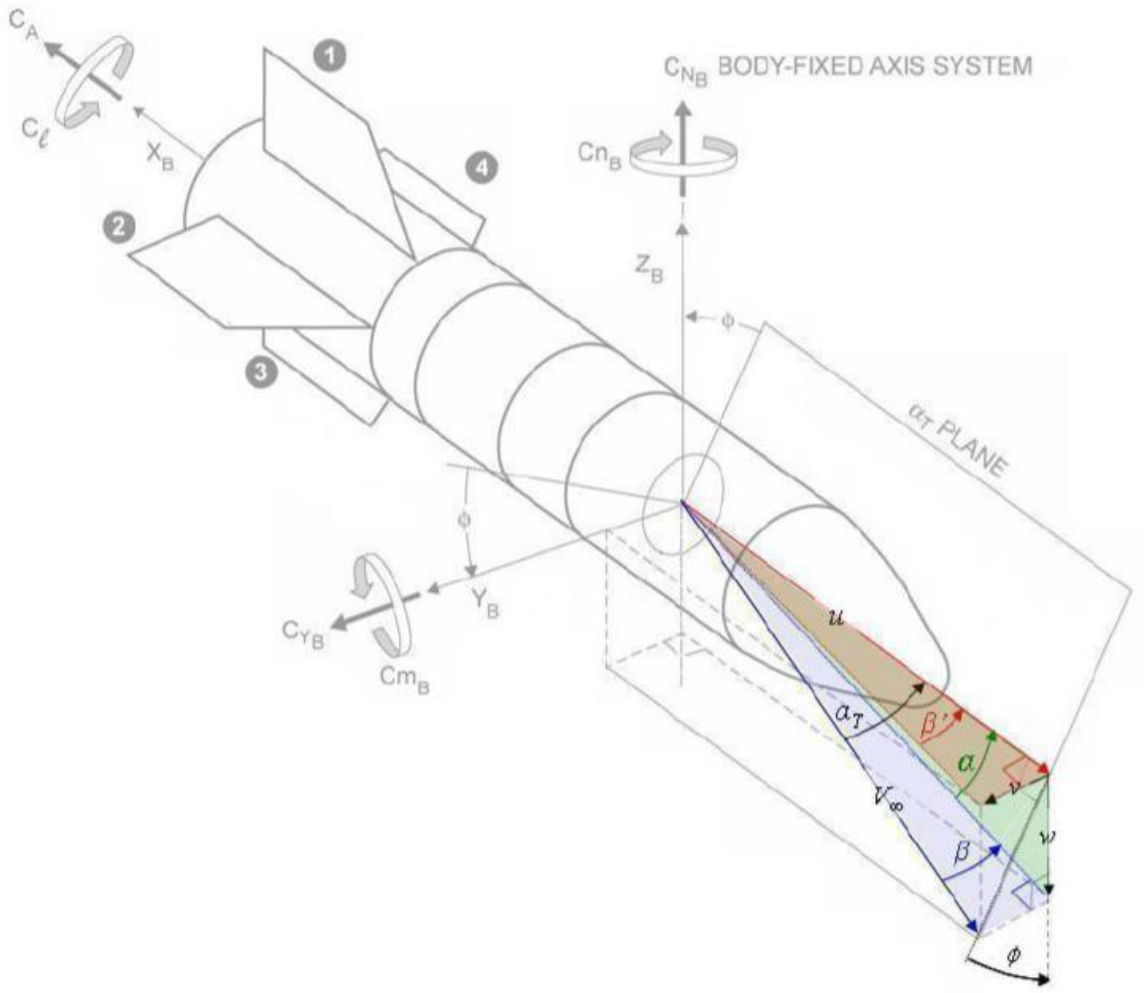

Figure 7. Axis Convention. Source: [34].

To make a missile navigate a turn, the force normal to the body axis (hereafter referred to as the normal force) provides the centripetal acceleration. The normal force can be generated by a variety of methods, either via

aerodynamics by means of control surfaces such as fins, or via thrust such as thrust vector control (TVC) or lateral thrusters seen on large rockets.

Therefore, instead of guiding a missile along a curved flight path, the missile's orientation can be abruptly changed through the application of forces to upset the stability of flight. Although aerodynamic control surfaces can be used, lateral thrusters or TVC is generally employed for this type of maneuver when a very rapid response is required, especially early in the flight when dynamic pressure is low. A dramatic example of employing this type of maneuvering is seen in Figure 8.

Figure 8. Example of Lateral Thruster Employment. Source: [35].

In the sequence of photos in Figure 8, the vehicle is provided an initial upward velocity. A lateral thruster near the front of the missile is then employed to initiate rotation of the vehicle. Once the vehicle is nearing an orientation approximately parallel to the earth, another opposing lateral thruster is fired to halt rotation. With the new orientation achieved, this particular vehicle then fires another, larger rocket motor to increase acceleration along its flight path. A similar effect can be achieved aerodynamically with pivoting control surfaces, although the required amount of dynamic pressure may not be available. However, the vehicle relies on a source of thrust in order to accelerate in the new direction. Therefore, this type of maneuvering is not applicable for periods of flight after motor burnout, which regime the SUAVE is expected to operate within.

Because the SUAVE is intended to be maneuverable after motor burnout and be low-cost, aerodynamic controls are considered. Actuated control surfaces come in many forms, and can be located at many positions along the vehicle body. Common missile fin layouts include combinations of rear fins, canards, and mid-body fins. The defining feature of any of these fin types is the location with respect to the center of gravity. Measuring from the tip of a missile's nose back to the center of gravity (CG), fins aerodynamic surfaces located between the nose and CG are called canards. Fins located very nearly at the same location as the CG are mid-body surfaces (aka fins, wings, etc.), and fins aft of the CG are rear fins. Using actuated aerodynamic surfaces allows control to be maintained after motor burnout, which is important for the SUAVE application.

2. Simplifications to a Constant Radius Turn

In accordance with the Fleeman design process, one must establish baseline performance, and then complete a full design iteration in order to determine if the baseline performance is met. To begin analysis, the short range intercept is modeled in a simplified fashion to establish baseline performance objectives. The flight path is envisaged to be a constant radius turn from the

launch plane to an intercept location located on the same plane as shown in Figure 9.

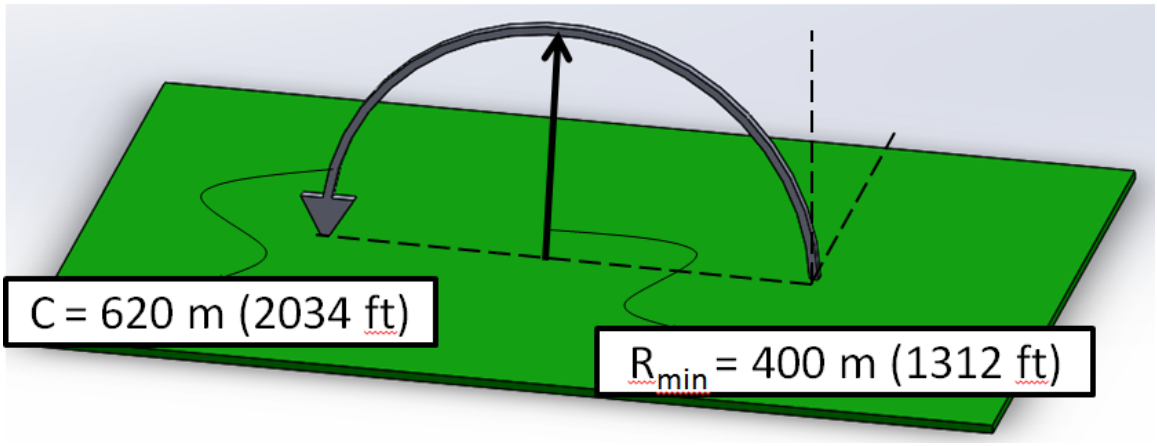

Figure 9. Intercept Flight Path Approximation

We can set a radius of turn and a minimum time from launch to intercept. If the distance at initial detection is assumed to be 500 m (1640 ft), the required radius is determined such that the intercept must occur at some distance closer to the launcher to account for falling debris (including uninitiated munitions). This distance is assumed to be 400 m (1312 ft). The radius of the turn is therefore 200 m (656 ft), and the distance of a 180° constant radius arc, denoted as C, connecting launch and intercept points is $C = \pi r = \pi * 200$ m = 628.3 m (2061.4 ft).

With the flight speed of the small UAV given in Chapter II. Sec A. Subsec. 3. Threat Performance Metrics, the small UAV will cover the difference between detection distance and desired intercept distance in 4.3 seconds.

Assuming that the SUAVE system can process a detection signal and launch the SUAVE in 1 second, then the SUAVE must close with the target UAVs by covering 628.3 m (2061.4 ft) in 3.3 seconds. Assuming constant speed throughout the turn (which ignores initial acceleration for the initial review and setting of design goals), the design speed during the turn maneuver is 190.4 m/s

(624.7 ft/s). As the intercept is low altitude, the speed of sound is taken as 340.3 m/s (1116.5 ft/s) [36], and so the associated Mach number is $M = \frac{u}{c} = \frac{190.4\ m/s}{340.3\ m/s} = 0.56$.

Additional quantities associated with this simple model can be explored with Newtonian physics. For a constant rotation at constant velocity, the centripetal force is defined as “a force that makes a body follow a curved path. Its direction is always orthogonal to the motion of the body and towards the fixed point of the instantaneous center of curvature of the path.” [37] The centripetal force can be equated with the rate of rotation, the radius of curvature, the desired velocity, and the mass of the object which is trying to traverse this arc. Assuming a mass of 35 kg (77 lbs) (this value is the result of much work which is discussed later, but is included here for cohesiveness of this report) and using the other values discussed in Chapter II. Sec. F. Subsec. 2. Simplifications to a Constant Radius Turn, the centripetal force requirement is

F_C=(mv^2)/r=((35 kg)*(190.4 m/s)^2)/(628.3 m)=2019.5 N (454 lbf) [38].

3. Mechanics of a Constant Radius Turn

To execute the desired flight path and flight conditions, the vehicle must generate the required centripetal force, as displayed in Figure 10. The aerodynamic forces increase as the square of the velocity; the centripetal force also increases as the square of the velocity, but remains a small proportion of the required force. In order to generate sufficient centripetal force, it is hoped to employ the motor thrust in addition to the aerodynamic force. The missile body itself will create normal forces once set at an angle of attack, in addition to any other aerodynamic surfaces. By moving the body to an angle of attack, the thrust vector can also be analyzed as consisting of a both a component tangential to the radius of the turn, and a component in the radial direction. This last is effectively centripetal force. The body should therefore be set at an angle of attack where the body force and radial thrust vector together generate the

required centripetal force, and where the tangential thrust vector is equal to the drag incurred at that angle of attack.

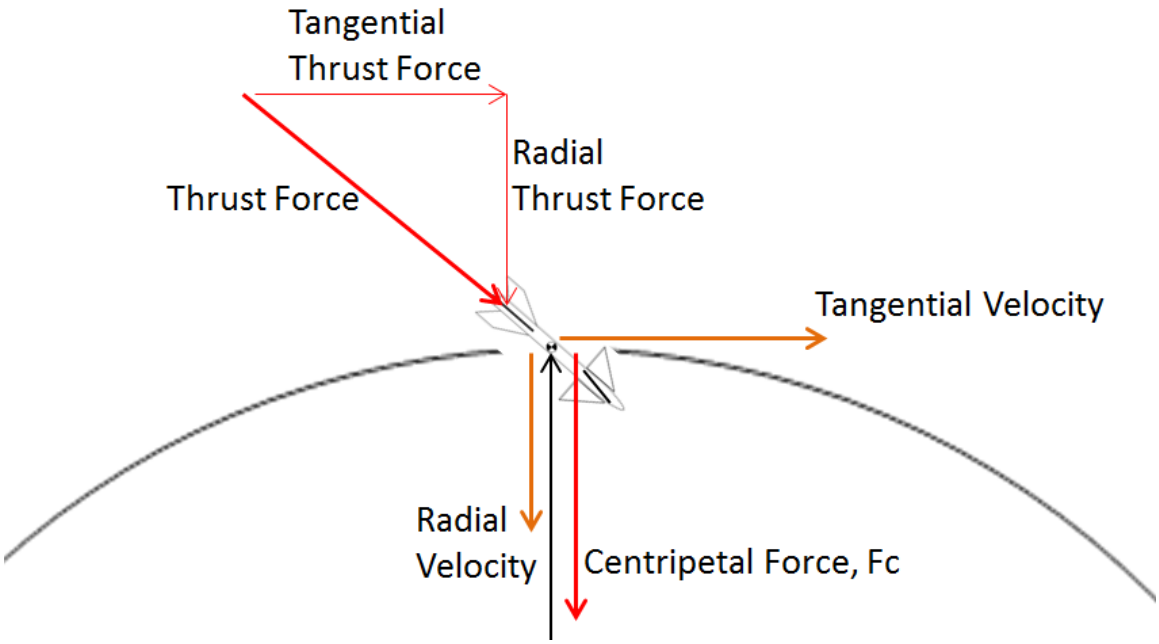

Figure 10. Intercept Flight Path Force Analysis

The aerodynamic forces come from the nose and body, the canards, and the rear fins. These, together with the thrust forces, are shown in Figure 11. Aerodynamic forces are in green and orange and thrust is in red.

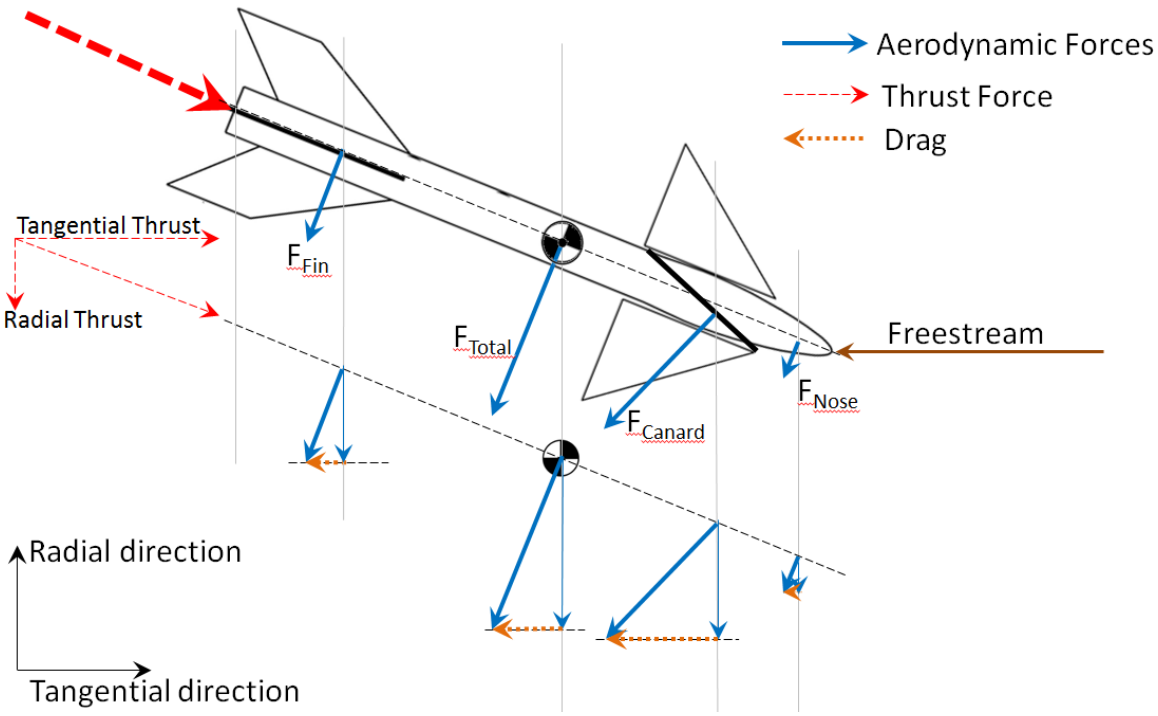

Figure 11. Vehicle Generated Forces and their Decomposition

Reviewing Figure 11, it should be noted that the drawing is not to scale; the canards especially are shown enlarged for clarity. The upper drawing is a rendition of the canard controlled vehicle, showing the approximate direction of the forces being generated when the flight vehicle is at some angle of attack relative to the freestream, depicted as the light blue arrow. The aerodynamic forces are assumed to be normal to the surface which is generating them, which is consistent with Missile Lab's body centered reference frame. The canard force is depicted as normal to the canard. The second depiction, the dashed line, shows the forces decomposed into tangential (horizontal in the figure) and radial (vertical) components. To maintain a constant radius turn, the tangential (horizontal) aerodynamic forces (the orange arrows) must equal the tangential thrust component. The radial (vertical) vectors, summed, represent the total centripetal force generated by the vehicle at a given flight condition.

G. PAYLOAD INTRODUCTION

As discussed earlier in Chapter II, Sec. B, Defeat Concepts, a small UAV has low vulnerability to many common weapon types. Determining the recommended payload for the defeat of small UAVs therefore requires research beyond the scope of this thesis. In order to continue the SUAVE development to prove the feasibility of the low-cost missile concept, a representative payload is being used.

A payload concept for the defeat of multiple small UAVs involves releasing guided submunitions from the SUAVE. It was assumed that the submunitions would require a large internal volume, and therefore a body tube of 191 mm (7.5 in) internal diameter was selected. The length of the payload section is similarly unknown, and therefore it was decided to mesh the requirements of the prototype vehicle with the expectations of an eventual production vehicle. Specifically, the prototype vehicle is required to be recoverable in order to constrain development costs, and therefore houses a parachute system. It was decided that to commence vehicle development, the volume and weight requirements of the parachute system would be a representative payload for the eventual production vehicle.

III. PROTOTYPING VEHICLE

Modern aerospace development is expensive [39], [40], [41], [42], [43], [44]. In an effort to control development cost, this effort intends to use COTS components, reusable development vehicles, and a focus on meeting minimum performance requirements. For a missile-like system to be reusable, design methodology employed in amateur rocketry is extensively borrowed. This includes the use of amateur rocketry recovery systems, specifically parachutes in this case. Amateur rockets deploy parachutes during their flight to allow the components to come down to earth in a controlled fashion.

THIS PAGE INTENTIONALLY LEFT BLANK

IV. DESIGN STEPS

The specifics of design activities related to each of Fleeman's missile design steps, and other steps as required, are discussed in this section. The development paths will follow Fleeman's steps as much as possible. This section will also serve as a record of quantities in order to aid follow-on activities.

A. ESTABLISH BASELINE

1. Storage Requirements

The vehicle is intended to launch vertically from a mobile storage container. It is hoped that the vehicle's max span (measured from fin tip to fin tip perpendicular to the missile longitudinal axis) will be limited to twice the body diameter. It is expected that this will provide sufficient fin semi-span so as to allow efficient control of the vehicle. With the current vehicle external body diameter of 197 mm (7.75 in), the fin semi-span is limited to 98 mm (3.875 in), and the entire span limited to 394 mm (15.5 in) as shown in Figure 12.

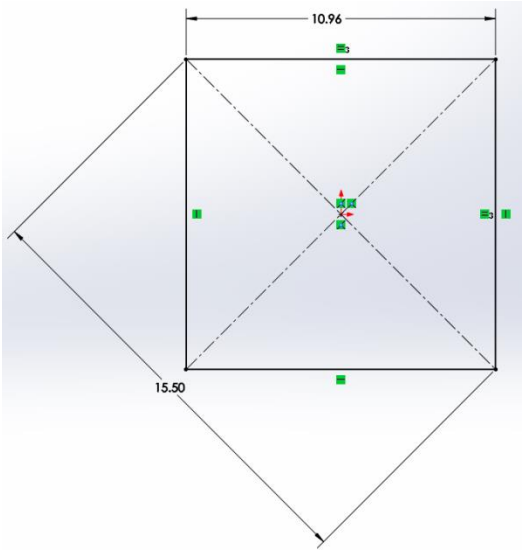

Figure 12. Representation of the SUAVE's Proposed Storage/Launch Container

2. Kinematic Performance Requirements

The current kinematic performance requirements are those necessary to execute the short range intercept of the expected small UAV threat, given assumptions regarding capabilities and detection ranges outlined in earlier sections. Summarized, these values are the distance between the SUAVE and target at time of detection taken as 500 m (1640 ft); the minimum distance between launch location and target intercept to avoid debris damage as 400 m (1312 ft); and the maximum time available to conduct intercept after launch as 3.3 seconds. The result of these values is shown in Figure 13.

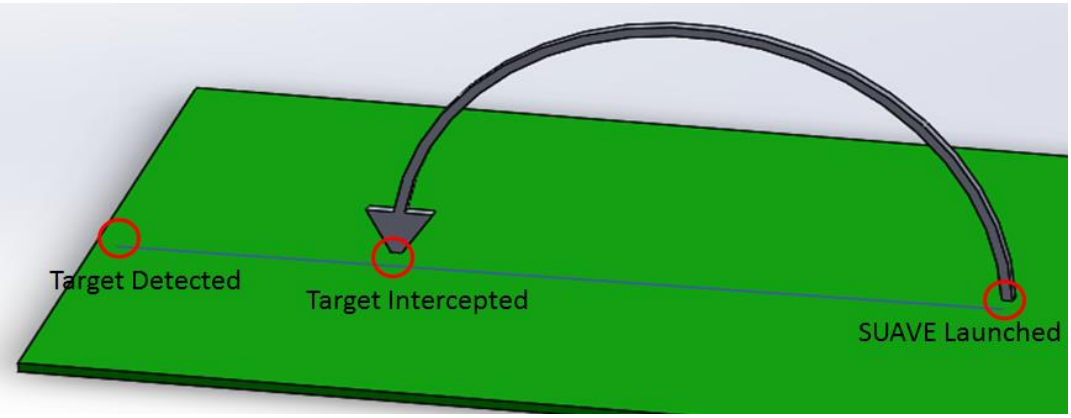

Figure 13. SUAVE Engagement Ranges

By using these criteria, the various SUAVE system elements' performances can be balanced to achieve a vehicle which meets the program intent.

3. Automation

The SUAVE system is intended to provide an automated defensive capability. All sub-systems must therefore be capable of performing their functions without operator input, other than maintenance at regular intervals. The maintenance requirements and detection system are outside the scope of this thesis, which focuses on the flight vehicle portion of the SUAVE system.

The prototype vehicle is intended to display the capability to navigate to a coordinate set independently after launch. Input data for the missile to achieve this function prior to launch is a coordinate set of both the SUAVE itself and the target, representing the location to which the missile must navigate itself.

4. Recoverable

The prototype is intended to allow three launches in a single day. The prototype must therefore require minimal maintenance between flights.

5. Short Turn Time

The prototype must be able to be made flight ready with less than 1.5 hours preparation work. This time period is from when the rocket is brought back from its landing site after a launch, to when it is posed on a launch rail and ready to launch.

B. PAYLOAD

It is assumed that the payload requires a 191 mm (7.5 in) internal diameter, 508 mm (20 in) long cylindrical section. It is further assumed that the weight of all recovery equipment (parachutes, CO_2 system, electronics and batteries) will be equivalent to the final weight of the payload.

C. AERODYNAMICS

1. Nose Cone

Nose cones affect the vehicle's aerodynamics and space requirements [32]. The required nose cone fineness for aerodynamic considerations is related to the maximum supersonic speed. Higher Mach numbers require finer nose cones for efficient performance. Subsonic applications do not require a cone, and perform well with a dome. If a seeker system is incorporated, a dome induces the minimum distortion in the information gathered by the seeker. There is therefore a trade-off based on the intended application.

The SUAVE is intended to not have an onboard sensor in order to reduce the vehicle cost, and therefore sensor distortion is not a consideration. In the

intended subsonic flight regime, a domed nose is sufficient from a drag consideration. The domed nose is the shortest of the recommended nose types, and therefore offers packaging and storage advantages. For this reason, it is the recommended nose type for the SUAVE application. Reviewing the COTS nose availability, a domed nose with a nominal 197 mm (7.75 in) external base diameter was not found to be available, and so a secant ogive offered by Public Missiles was chosen instead. A dome should be COTS sourced and installed prior to any aerodynamic testing intended to refine the final design.

2. Canard Rationale

Several methods of aerodynamic control are available. Each method is defined by what surfaces are used along the missile body to alter the vehicle's orientation. The question of which surfaces are controlled influences the details of the motion of the vehicle. Any aerodynamic surfaces across the body can be actuated to induce a moment about the center of gravity for the vehicle and therefore result in a change of the missile's orientation. Each configuration offers advantages and disadvantages. After a review presented in the 2017 ME4704 Course Report by ENS Schnabel [45], canards were chosen to provide control of the missile's flight. For the SUAVE application, which is desired to have control both during and after motor burnout, and be able to provide turning performance at low speeds, canards have been decided upon for evaluation. Tail control is very common, but is not expected to perform well at providing tight radius, low speed turns. This is because a rear fin controlled design requires the rear fins to generate forces away from the direction of the turn to pivot the vehicle toward the turn, at which time the body attains an angle of attack and generates aerodynamic force in the direction of the turn. This method of achieving a turn incurs a delay in response as the vehicle initially translates in the direction opposite that intended, until such time as the aerodynamic force generated by the body overcomes the fin force and directs the vehicle in the intended direction. This is a less efficient maneuver relative to canard control as the fin force remains opposite to the desired radial force direction. Tail control requires only

one set of fins, which reduces overall drag and can therefore extend range, but at the expense of minimizing turn radius. Mid body fins are more suited for long range, low turn rate applications. Canard control allows the vehicle to be placed at an angle of attack relative to the freestream airflow, at which point all the aerodynamic surfaces (including the body) generate aerodynamic forces with significant components oriented in the centripetal direction. This creates an efficient aerodynamic layout, which it is hoped will offer superior performance for both turning and long-range intercept energy management.

Figure 14 shows a missile with actuated canards. The canard fins are deflected so as to maneuver the vehicle by causing rotation about the CG; ultimately the rear fins create a restoring force which balances the upsetting force from the canard fins and allows the vehicle to adopt orientations where all moments are balanced and the body is not rotating, called trim points. For a functional design, canard fin deflections and body angle of attack require quantification. An analysis of the motion due to a similar deflection of opposing canard fins provides some insight into what angles are appropriate for design targets.

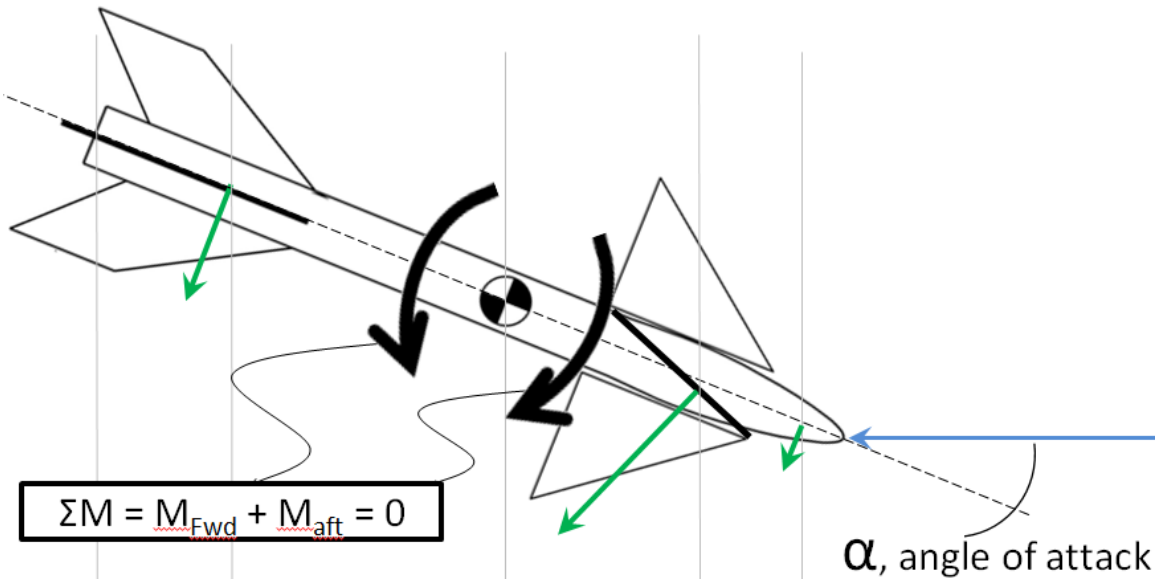

Figure 14. Vehicle Free Body Diagram for Trimmed Flight

3. Canard Missile Free Body Diagram

Because the canards are sized to the available torque of the actuators, the rest of the vehicle's aerodynamic layout is designed to allow the vehicle to rotate up to a 15 deg angle of attack. This is done by first identifying all the required components. Next a component layout with approximate sizes is created. With knowledge and/or assumptions regarding the weights of each component, the overall weight and center of gravity location can be determined. The rear fins are then bounded to an aft location, which is almost inevitably the rearmost available position. Armed with all these values, the rear fins can be sized. Unfortunately the accuracy of the fin size is directly related to the uncertainty of the values for vehicle length and weight which have been used as input to the model. It is recommended that the model providing the vehicle mass properties is refined as much as time allows before a rear fin is chosen, so as to achieve the highest accuracy in fin design and sizing possible. This represents iteration within Fleeman's Missile Design cycle, as the design becomes further and further refined.

Any body rotation will add to that already commanded by the canard, so that the canard sees its own rotation plus that of the body. Ideally, the canard planform will continue to provide lift until some very large angle of attack, perhaps 45 or more deg. A limit is caused by the orientation of the normal vector relative to the body; after 45 deg, a constant vector offers less force normal to the body, and more force axial to the body (and therefore not useful). For controllability, it is desired that when the body is at a specific angle of attack, the canard's angle of attack be a certain amount of the range in which the canard's normal force continues to increase with increasing angle of attack. The deflection angle of the canard to achieve the desired vehicle angle of attack must be sufficiently large to avoid undue sensitivity to canard deflections (a balanced set of fore/rear forces to adopt max body angle that includes only a small difference between canard and body means that a free-stream perturbation will greatly affect the flight profile, and that small adjustments of the canard angle of attack will cause large adjustments of the body's angle of attack. This last is related to

the accuracy of the control system, specifically if it can accurately and quickly position the canard in relative angle to the body). It is therefore decided that the canard is required to move approximately 20% of its max useful range to cause the body to adopt the desired angle of attack.

The canard's angle of attack, when the body is at the maximum desired body angle of attack, should be some percent of the canard's region of angle of attack wherein the lift continues to increase with increasing angle of attack, so as to ensure control authority. "Control authority" means that greater canard normal force is available at the desired body angle of attack so that the forward forces can overcome unexpected anti-rotation forces. 75% of the canard's range of increasing normal force relative to angle of attack is chosen as the design target for canard fin angle of attack at the time that the body has adopted its highest angle of attack.

The canard's angle of attack is further limited in two ways: useful aerodynamic range, and mechanical range of motion. The useful aerodynamic range can be defined via ENS Schnabel's review [45] via MissileLab of the lift qualities of the canard planform selected. Previous review of this work indicates that 32 deg seems to be the realistic maximum (therefore, $\alpha_{canard\ max}$=32 deg). Using 75% of the useful range provides us with $\alpha_{canard\ max}$=0.75*32 deg=24 deg. Mechanical range of motion is currently set by the servo's range of motion and the reduction ratio used to maximize the torque while continuing to respect the 150 deg/s suggested limit. As the servos have a range of +/-90 deg, with a 3.5:1 reduction, they can only turn 25.7 deg.

The desired body's angle of attack would likely be about 45 deg, if not otherwise constrained. The other constraint is the canard's angle of attack (α_C), which is the sum of both the body's angle of attack and the canard's deflection relative to the body axis (δ). δ_{max} is the maximum canard deflection relative to the body at which the body will adopt its desired angle of attack (constrained by the canard's maximum α_C). α_{body} is the body's angle of attack due to canard constraints. Because the canard must be deflected relative to the body in order

for the body to assume an angle of attack, the canard will always be deflected relative to the body, and the canard normal force generated will be a product of the cosine of the canard deflection angle. Since cosine equals 1 at zero deflection, and decreases to a value of zero at 90 deg, smaller angles are preferred. Practically, over 90% of the canard normal force will be normal to the body axis if δ is kept below 25.8 deg; the 95% threshold is 18.2 deg. Therefore, this effect can be ignored so long as the fin deflections are kept less than 18 deg. A useful relation between canard angle of attack, canard deflection, and body angle of attack for determining the final α_{body} is:

$$\alpha_{body} = \alpha_{canard} - \delta_{design}$$

δ_{max} should ideally be determined by an analysis of the dynamic response of the body to an expected airflow perturbation; specifically that for a perturbation of the freestream of some angle, amplitude, and duration, that the system will seek its static equilibrium with an acceptable deviation in heading and position. Without doing this analysis, δ_{max} will be set by assuming a value of 9 deg.

Assuming that 9 deg of canard deflection allows a comfortable range in which disturbances will not unduly upset the vehicle and the canards may retain control authority, then the expected body angle is:

$$\alpha_{body} = \alpha_{canard} - \delta_{design} = 24 - 9 = 15 \text{ deg}$$

As an upper limit to $\alpha_{body\ designed}$, if the canard were used more aggressively:

$$\alpha_{body} = \alpha_{canard} - \delta_{design} = 30 - 4 = 26 \text{ deg}$$

A review of national advisory committee for aeronautics (NACA) airfoils [46] shows no symmetric airfoils which produce useful lift above 16 to 18 deg angle of attack; this makes the α=26 deg target with a conventional airfoil extremely unlikely. Instead, planform effects (such as a delta's vortices creation) are used to achieve a high L/D over a useful range of α that extends past 20 deg, and these planform effects are produced by both flat plates and airfoil sections.

This allows greater effect from the use of a flat plate. Use of a flat plate is advantageous because it simplifies manufacture and reduces cost.

4. Actuator Selection Impact

The actuators used to deflect the canards are an important driver to the overall design, specifically the aerodynamic control surfaces. An ideal actuator is lightweight, compact, can provide actuation for the expected maximum flight time with an acceptable margin of error, and low-cost. The actuator determines the parameters of the control surface, because the torque generated by aerodynamic forces on the control surface cannot be allowed to exceed the stall torque of the actuator, or control authority of the vehicle will be lost. The control surface's performance in turn governs the maximum attainable angle of attack, which dictates the maximum vehicle turn rate.

An actuator subsystem has several important characteristics, such as weight and volume, and the duration which is the amount of time that the actuator can continue to apply force and is a function of the energy consumption rate and the amount of energy available. Some systems, such as gas generators, use their own expanded combustion gases to power an actuator, and will have a finite operating duration once ignited before they burn out. Other systems, such as electric motors or pneumatics with a fixed reservoir, also have a finite amount of energy available for the execution of control surface deflections. Most aerodynamic surfaces will experience increasing amounts of aerodynamically-induced torque as they generate more normal force. Therefore, the actuator torque must exceed the expected aerodynamic torque in order to maintain control authority while maintaining an acceptable turn rate of the control surface. Fleeman recommends a minimum turn rate of 150 degrees per second [32]; rates of 300 – 400 degrees per second are recommended for high performance vehicles. Actuator torque and turn rate can be traded via gearing.

5. Actuator Selection

Servo options were reviewed as part of the 2014 ME4704 course [47]. Upon commencement of the project which is covered by this thesis, the actuators selected were Futaba BLS-172SV servo motors [48]. As the capability of servo motors and other actuators is constantly improving, it is recommended to revisit this selection in support of future work.

Futaba BLS-172SV servos are approximately $219.99 [48]; at the highest recommended voltage, they provide 3.63 Nm (514 oz-in) torque at 546.45 deg/s. To maximize the available torque, reduction gearing is employed. Respecting the minimum turn rate of 150 degrees per second, a speed reduction of 3.64:1 can be used. Reviewing the available COTS gear sets, a 3.5:1 speed reduction was employed, providing 12.705 Nm (1799 oz-in) of torque. Applying a Safety Factor of 1.2 to the available torque, the available design torque is 10.164 Nm (1430 oz-in), delivered at 156 deg/s over a range of +/- 25.7 deg from the neutral position.

6. Actuator Assembly

The actuators require an assemblage to rigidly hold the servo motors and gearing while transmitting torque to the control surfaces. With canards chosen for the control surfaces, and the 191 mm (7.5 in) internal vehicle diameter limiting available space, a design was created with the intent of achieving ease of manufacture, low cost, and low weight. The entire internal body diameter was deemed available for the actuator assembly, and no effort was made for an internal passage through the actuator assembly.

Previous iterations of actuator mountings and assemblies had been implemented by ME4704 course efforts. Unfortunately, these early iterations suffered from loose mechanical connections at each of several mechanical joints such that the actuator motion was not accurately transmitted to the control surface. The loose constraints of the control surfaces resulted in movement under aerodynamic forces away from the intended position. It was decided to redesign, rather than iterate, the actuator assembly.

The general concept of the new actuator assembly was to provide a pivoting shaft, upon which the canard fin and the gear would be mounted. The shaft would be supported by a bearing as close as possible to the fin (the outer bearing), and also at the far end of the shaft (the inner bearing). The bearings and actuators would be supported and held in geometric relation by a rigid structure. It was further decided that the structure would itself slide into the body tube, and that the canard fins would each attach to the end of the shafts by a small length of cylinder inserted through the body. This allows the actuator assembly, once the fins and electrical connections are removed, to be itself removed from the body as a complete assembly. Required work can then be performed with ease of access to the assembly.

One of the design goals of the actuator assembly was to minimize bearing loads by avoiding or minimizing a cantilever load. If the span-wise center of pressure of the canard's fin planform is located at a distance from the centerline of the outer bearing greater than that of the distance between bearing centerlines, then the canard fin's aerodynamic force transmitted to the bearings is amplified. This is illustrated in Figure 15.

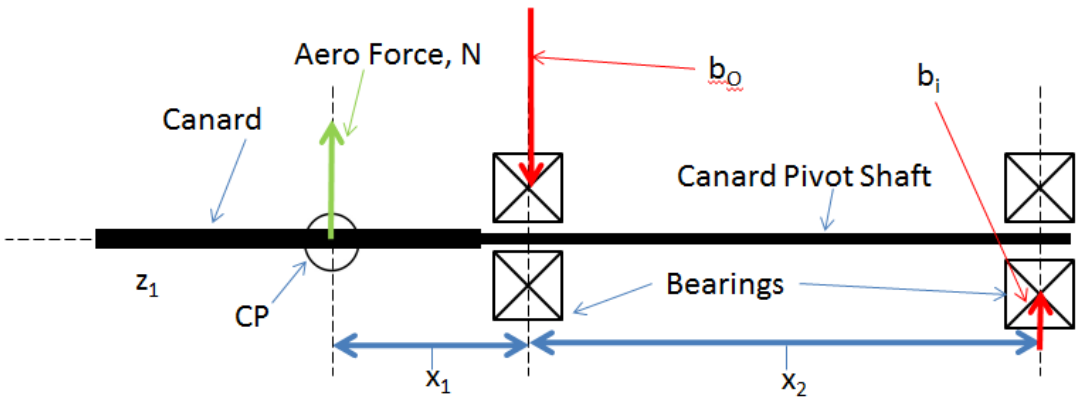

Figure 15. Actuator Force Analysis

By considering Figure 15 as a statics problem and taking moments about fixed points, the effect of varying distances x_1 and x_2 can easily be seen in

equation form, where b_i is the load on the inner bearing; b_o is the load on the outer bearing; x_1 is the fin's center of pressure (CP) to outer bearing centerline distance; x_2 is the outer to inner bearing centerline distance; N is the aerodynamic force normal to the fin's surface; and z_1 is the fin's semi-span (unused here).

$$b_i = N*x_1/x_2 \text{ ; and } b_o = N*(1 + x_1/x_2)$$

Therefore in order to maximize the rigidity of the structure under flight loads, it is preferred for the outer and inner bearings to be spaced as far apart as is practical. Current constraints on fin semi-span place the span-wise center of pressure at approximately 32 mm (1.25 in). The outer to inner bearing centerline distance is 73.8 mm (2.906 in). Therefore, the canard fin center of pressure can be comfortably moved further from the body so long as aeroelastic effects are continued to be ignored.

The bearing surfaces are also important. They must bear the forces b_o and b_i in Figure 15, allow rotation of the pivot shaft, and produce the minimum friction. Because of the actuator's torque limitations and the semi-span constraint, the maximum force of the canard fin is relatively low at 111.2 N (25 lbf) at maximum design flight conditions. Therefore, ball roller bearings can be used in this application. The coefficient of friction for ball roller bearings is 0.0015 [49]. Therefore, the friction was omitted from further considerations. Note that if the x_1/x_2 ratio were made much greater than 1 and the normal force increased by means of a large semi-span canard fin, the bearing friction may become significant relative to the available actuator torque.

The actuator assembly structure was a laser-cut sheetmetal weldment. Use of laser-cut sheetmetal allows several advantages. Sheetmetal itself is less expensive than billet, casting, or forging. Laser-cutting is a relatively inexpensive metal cutting operation, that allows cutting of any 2-dimensional shape to close tolerance. This allows complicated curves and interlocking segments to be rapidly produced. 3-dimensional structures can then be assembled from

interlocking flat components and welded together. This provides a relatively easy method of creating structures that meet the core objective of all structures: placing material where it is needed, and leaving air everywhere else. Best achieving that objective requires complex 3-dimensional shapes to resist 3-dimensional loads, which are more time consuming and costly to otherwise create. Laser-cut sheetmetal weldments offer less ideal grain-flow than complex stampings, but do not require the large investments in tooling and procedure development. Complex milling operations have a limited range of shapes available due to the requirements of tool access, and generally incur greater costs in tool wear and set up time. When employing laser-cut sheetmetal weldments, care must be given to tolerancing, welding access during welding/ assembly, and heat affected zones from the welding.

The sheetmetal used was 17–4 stainless of 0.8 mm (0.032 in) thickness. The thickness was chosen based on engineering intuition and experience in the interest of striking a balance between weight, rigidity, and weldability. The 17–4 alloy is a high-strength stainless which suffers minimal distortion from welding.

Use of a fin pivot shaft with bearings affixed to the ends and driven by an actuator required mounting points for the bearings and for the actuator. The bearings were pressed into bearing pockets with integral screw mounting holes to allow affixing to the weldment. The actuator's pinion meshes with the shaft gear and neither require further support. The actuator itself was found to fit nicely into some pre-existing mounting brackets, which themselves were affixed to the weldment with screws through slots cut perpendicular to the plane of the gear. The geometry of these slots allowed adjusting the gear lash by moving the actuator closer or further from the gear/pinion axis centerline as shown in Figure 16.

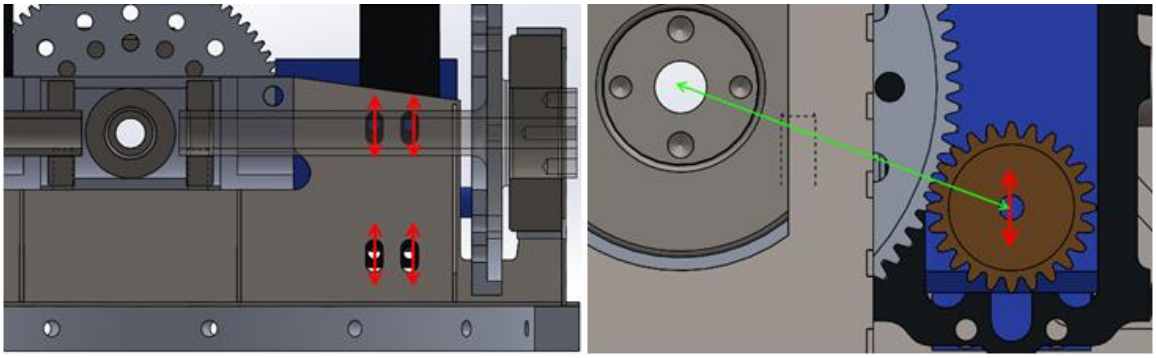

Figure 16. Gear Lash Adjustment

The inner bearing is a press fit in the inner bearing hub, which itself holds all four inner bearings. A sliding fit was used for the shaft to inner bearing interface to avoid additional axial bearing loads caused by flexure due to stress or heat of the structure or shaft. The outer diameter of the inner bearing greatly dictates the efficient usage of the missile's internal space, as all four inner bearings must fit in close proximity. This arrangement is seen in Figure 17. A point of improvement, especially if moving to canard fins with a significantly longer semi-span, would be increasing the distance between the outer and inner bearing centerlines by revisiting the positioning of the shafts and bearings.

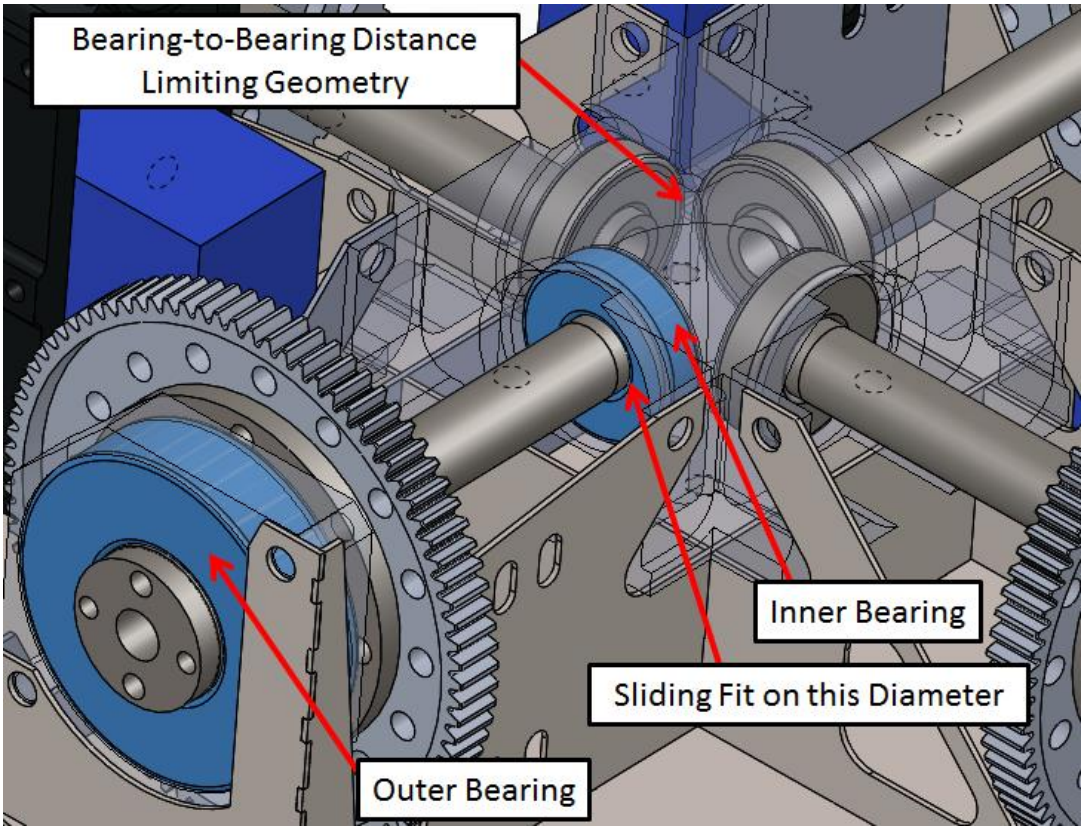

Figure 17. Bearings in Bearing Pockets in Bearing Retainers

Another recommended area of improvement is gear rotational position adjustability. The gear driven by the actuator pinion is mounted directly to the pivoting shaft. No special control of the rotational orientation of the gear was included. Neither was any facility to adjust the rotational orientation of the gear, canard fin, or pinion in relation to the actuator included. Therefore, there is no mechanical method of fine tuning the rotational position of the canard fin relative to the actuator. A method of fine tuning would allow setting the actuator at its neutral position (0 deg deflection), and ensuring that the canard fin is also at its neutral position (0 deg deflection). Since no such mechanical method exists, the components must all be assembled, and adjustments made in the software settings such that the canard fin is deflected away from 0 deg deflection. Failure to do so means that the system at rest will have the canard fins deflected and generating aerodynamic force during flight when none is required.

7. Discussion of Missile Aerodynamic Prediction Software

Analytic prediction of integrated missile aerodynamics is still not a well-refined science [31]. Several methods of predicting missile aerodynamics exist. None have been shown to offer perfect or near-perfect values. An aerodynamic prediction tool available is the U.S. Army's Missile Lab. This tool is a graphical user interface, which allows a user to define geometry, flight conditions, and a few other parameters. Once defined, these values are translated into inputs to several different aerodynamic prediction computer codes which are then run by Missile Lab (assuming that they are available, installed, and selected to be run). Missile Lab was designed this way because it is understood that the best implementation for missile aerodynamic prediction by computer code is to run several different codes and compare the results. This allows cross-comparison of the results of different prediction codes, from which it is hoped that the final values selected will be a more accurate reflection of the final product. The U.S. Air Force's Missile data compendium (DATCOM) is a FORTRAN code available to the Missile Lab graphic user interface, and accessing it through Missile Lab greatly increases the user-friendliness and decreases the time required for a user to become proficient with the software. It should be noted that Missile DATCOM is a predictive software, and not a perfect reflection of reality, and therefore predictive errors can be found. An example encountered by the author is the normal force generation of a fin which is heavily shrouded by the body due to the body's angle of attack; this particular case is not correctly modeled by Missile DATCOM. However, in general the code provides good approximations to experimental results [50].

Because missile aerodynamic prediction is not a perfect science, it is the intent to use flight testing of the prototyping vehicle to verify aerodynamic predictions. Software predictions are excellent as a design tool, but in no way supersede or supplant testing. Therefore, all aerodynamics must be validated by testing at some stage in the development program.

8. Canard Sizing

The size and shape of the canard fin has a huge impact on the vehicle tight-turn performance. The exact size and shape was investigated by ENS Schnabel as part of the 2017 2nd Quarter ME4704 course [45]. The results are summarized in the following text in order to provide reference information; please see the main report for details.

When considering a fin with a fixed pivot location, the motion of the center of pressure relative to the pivot point creates a moment arm. A fin with a long chord will see a greater moment arm, as the CP will traverse a greater distance over a given range of angle of attack than a shorter chord. By increasing the fin's semi-span, the size of the moment arm for a given fin area can be limited. This may allow a higher normal force from the canard fin for a given maximum torque at the actuator, which will improve the vehicle's ability with regards to the tight turn requirement. Because the design has very limited torque from its actuators, this CP moment arm is extremely important to this missile design.

Due to the actuator's torque limitations, the size and shape of the canard must be designed so that the surface's rotational moment cannot exceed the actuator's stall torque capability. The rotational moment for a specific set of flight conditions is a function of the CP to pivot axis moment arm, cross-sectional shaping, and planform. Using an airfoil shape for the fin's cross-section may show improvements in CP location changes, but at an increase in manufacturing cost. The current design uses a flat plate, as this is an easy to make cross-section, and it is hoped that this cross-section can meet the performance requirements. Analysis of the decrease in CP location variation vs manufacturing cost is recommended if it is found that a flat plate cannot provide the desired performance.

Altering the planform is very important to this design. The sweep angle is measured away from a theoretical reference that is perpendicular to the missile's longitudinal axis, to the line of the leading edge of the fin. Higher sweep angles

provide superior high angle of attack performance, at the cost of less aggressive lift vs angle of attack slopes. This vehicle is intended to attain a high angle of attack, and so the canard fin must provide a useful lift curve at high angles of attack. To meet the requirements of semi-span limitations, actuator torque limitations, and high angle of attack performance, the fin shown in Figure 18 was chosen.

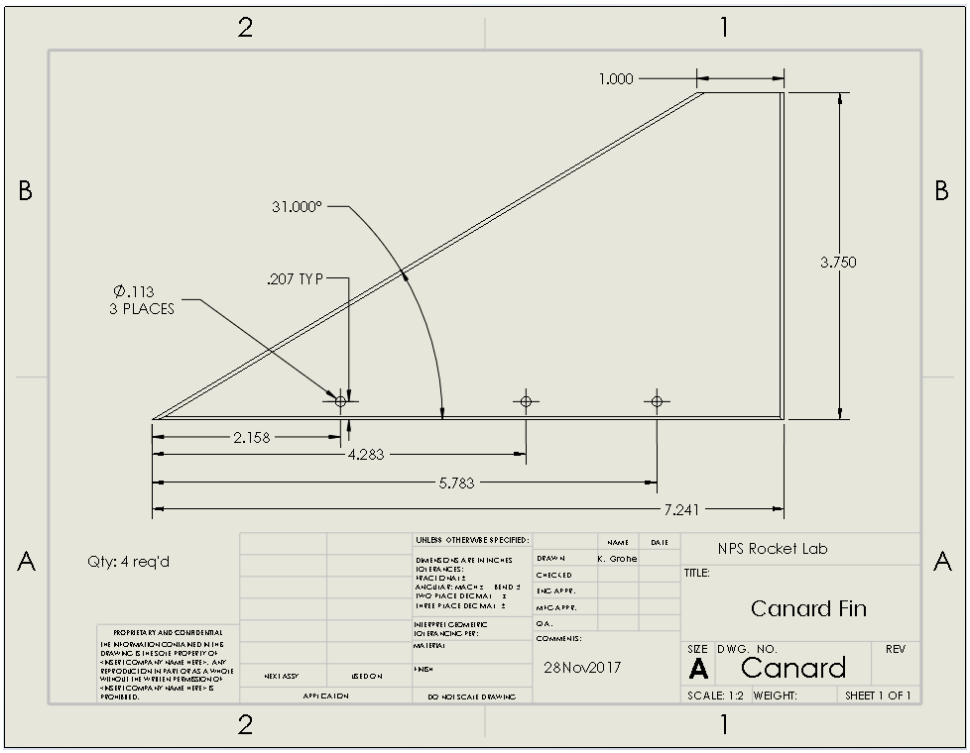

Figure 18. Canard Fin Selection

The material chosen for the canards is G10 fiberglass, which can be found commercially in pre-cut shapes and a selection of thicknesses [51].

9. Rear Fin Sizing

A 76/40 planform would offer a steep coefficient of normal force (CN) vs angle of attack slope relative to a pure delta [52]. A non-swept plate will seldom offer greater than 12 deg of angle of attack before stalling. Similar to the canard,

the expected angle of attack is greater than the useful regime offered by conventional symmetric airfoils. Pending more detailed analysis to optimize the L/D for the expected flight conditions, a flat plate delta planform is selected. Neglecting the body's aero force contribution, the tail fin's size and lift slope angle must be matched to provide

$$(dCN/d\alpha_{fin} > dCN/d\alpha_{canard} + dCN/d\alpha_{nose})$$

With a planform selected, the fin area is determined by balancing against the other expected aerodynamic forces, such as the canards at max designed angle of attack, and the nose, body, and transition at the designed body angle of attack. The desired fin will produce forces to balance the moments generated fore and aft of the CG. To do this, the location of the CG must be estimated and simulations of the body geometry run in Missile Lab.

With Missile Lab output accepted as sufficiently accurate to advance the design, the rear fin design is iterated until the vehicle is shown to have a negative (restoring) moment at 0 to 15 deg angle of attack, the ability to achieve a trim condition at a minimum of 15 deg angle of attack, and a margin of a minimum of 6 deg (this value is an assumption) after attaining a trim of 15 deg angle of attack wherein the vehicle has a negative restoring moment. To do so, it was initially thought to employ a rear fin with a delta planform, of sufficient area so as to provide an acceptable static margin when the canards are at 0 deg deflection. It was believed that a delta with sufficiently high sweep angle would allow the actual normal force to increase sufficiently gradually that appropriate deflection of the canards would upset the stability, and cause the body to adopt an angle of attack whereat the rear fin's moment about the center of gravity would balance that of the canards.

As aerodynamic force developed by a surface is a non-linear function of cross-section, planform, and aerodynamic interactions, the rear fin size and shape was iterated with Missile Lab to find a shape that provided the desired vehicle performance. For manufacturing concerns, no airfoil shapes were considered; all

fins were a flat plate. It was rapidly discovered that respecting the maximum semi-span of ½ body diameter was not possible. Delta planforms of various size and shape were tried first. Unfortunately, delta planforms of sufficiently high sweep angle to allow the adoption of high body angles of attack offered insufficient restoring moment for straight line flight. Lower sweep angles allowed stability for zero deflection conditions, but generated too much lift at higher angles of attack. A dual-delta, such as a 76/40 planform, allows the generation of lift at high angles of attack through the creation of a vortex at the join between the high-sweep forward delta and the low-sweep main wing section. At high angles of attack, this vortex ensures sufficient flow across the top of the airfoil so that lift is generated. It was eventually reasoned that the inverse of the 76/40 planform, as per Figure 19, would combine the high lift slope of zero sweep planforms and the large range of high sweep planforms. The hope was that a straight section of airfoil would provide a very aggressive lift curve at low angles of attack, but would stall early; and a high-sweep delta would provide high-angle of attack performance through vortex generation. By increasing the sweep, the lift slope is expected to decrease, thereby providing the delayed-onset lift required. Affixing the delta to the straight section keeps the vortex away from the straight, allowing it to lose lift after a certain angle of attack, while the high-sweep delta continues to provide (slowly) increasing lift at increasing angles of attack.

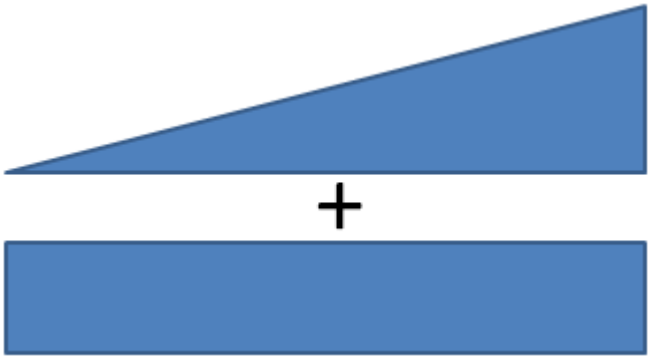

Figure 19. Rear Fin Planform Concept

This idea was first implemented in a configuration which offered a relatively conventional appearance of a straight fronted short section with a highly swept delta atop and then iterated as in Figure 20. This was found to offer an insufficiently aggressive initial slope for the lift vs angle of attack plot. To increase the low angle of attack lift slope, the semi-span of the straight section was increased and the chord reduced. The sweep angle was increased so that the lift slope from the delta would be very gradual. The delta section then required a greatly increased area to provide the correct amount of lift. As the delta section's chord exceeded that of the straight section, the tips of the delta were not allowed to end in sharp points, but were made flat in order to provide greater structural strength against rough landings. To guide design modification, the predicted lift curve for select planforms was plotted, as seen in Figure 21.

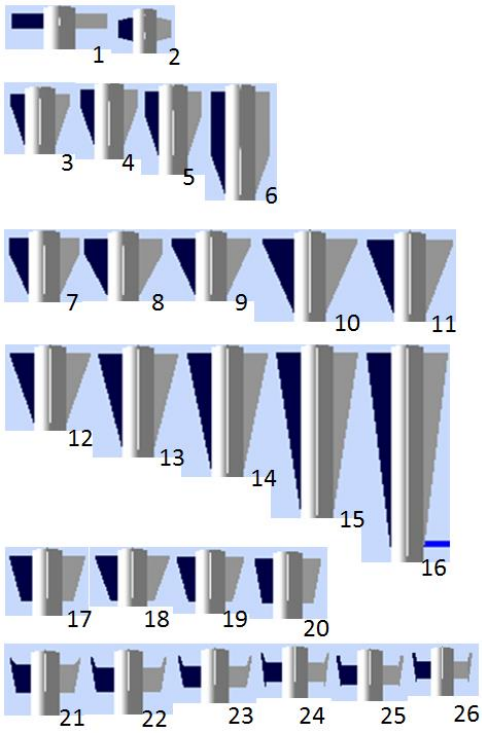

Figure 20. Canard Design Iterations

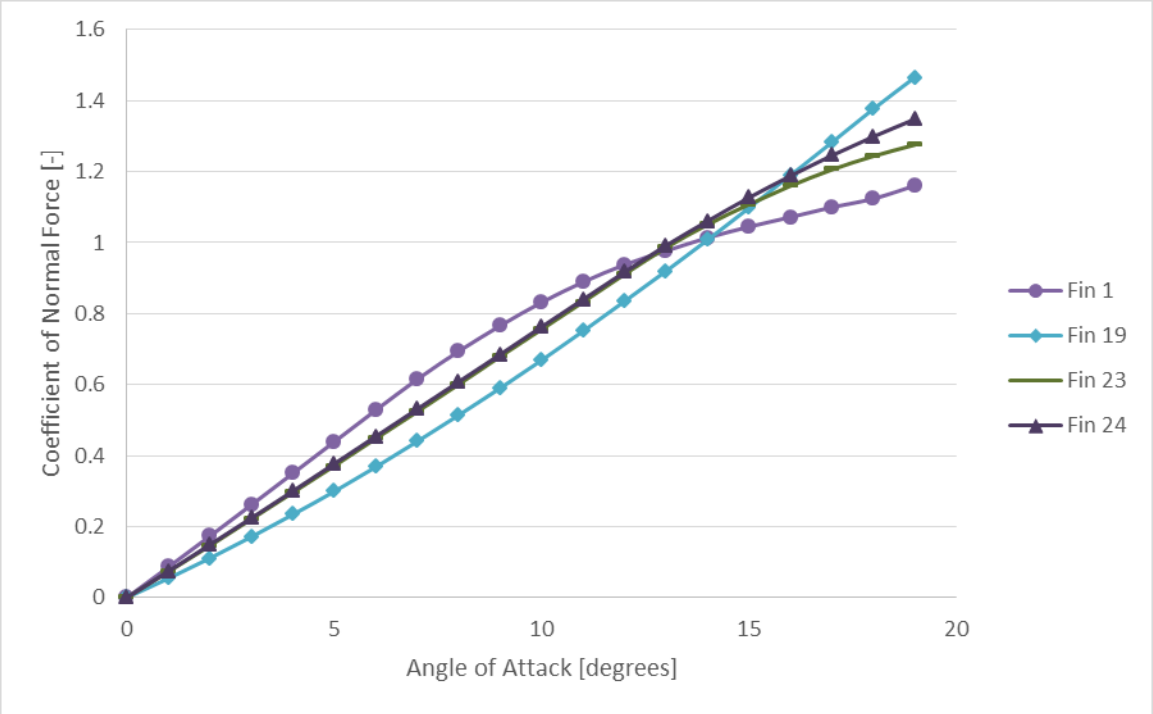

Figure 21. Static Aerodynamic Characteristics of Several Fin Planforms

The general trend for planforms of the delta affixed to equal chord length zero sweep section style is a lift curve which continues to climb steadily around the 15 deg point of interest. Fin 20 is the last geometry of the equal chord length style tested. With fin 21 the delta's chord is larger than the chord of the zero sweep section, and the lift slope can be seen to decrease with increasing angle of attack. After several further iterations, it was found that the specific geometry of the general "long and thin semi-span topped by large delta" concept shown in Figure 22 offered a lift slope that in conjunction with the estimates of body geometry and weights, met the desired performance characteristics. The final iteration included alterations to avoid sharp points and particularly thin sections in the hopes of avoiding structural problems.

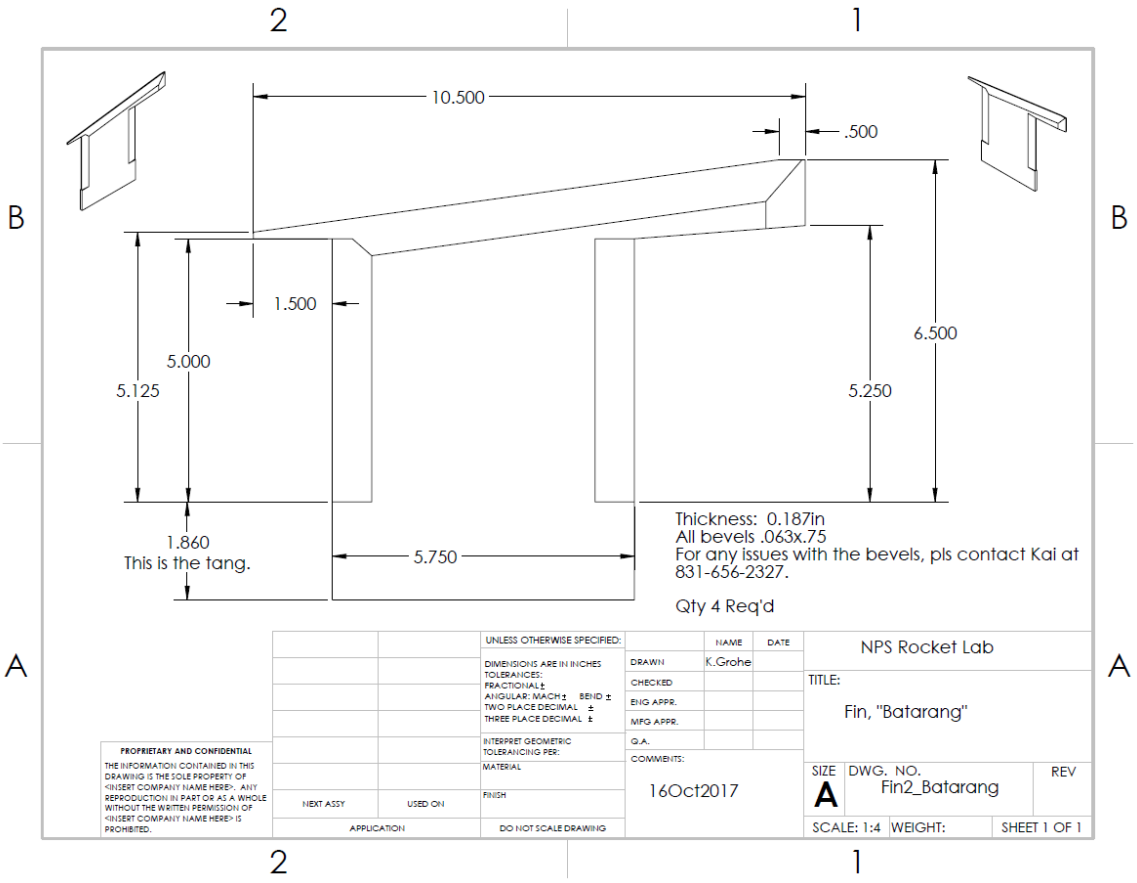

Figure 22. Rear Fin Selection

With the chosen fin, it has still not been determined if the vehicle is dynamically stable (see Figure 23). However, with an aerodynamic layout that meets the initial criterion of allowing the desired angle of attack and static stability chosen, it is recommended that the dynamic response be investigated as the next step in aerodynamic design.

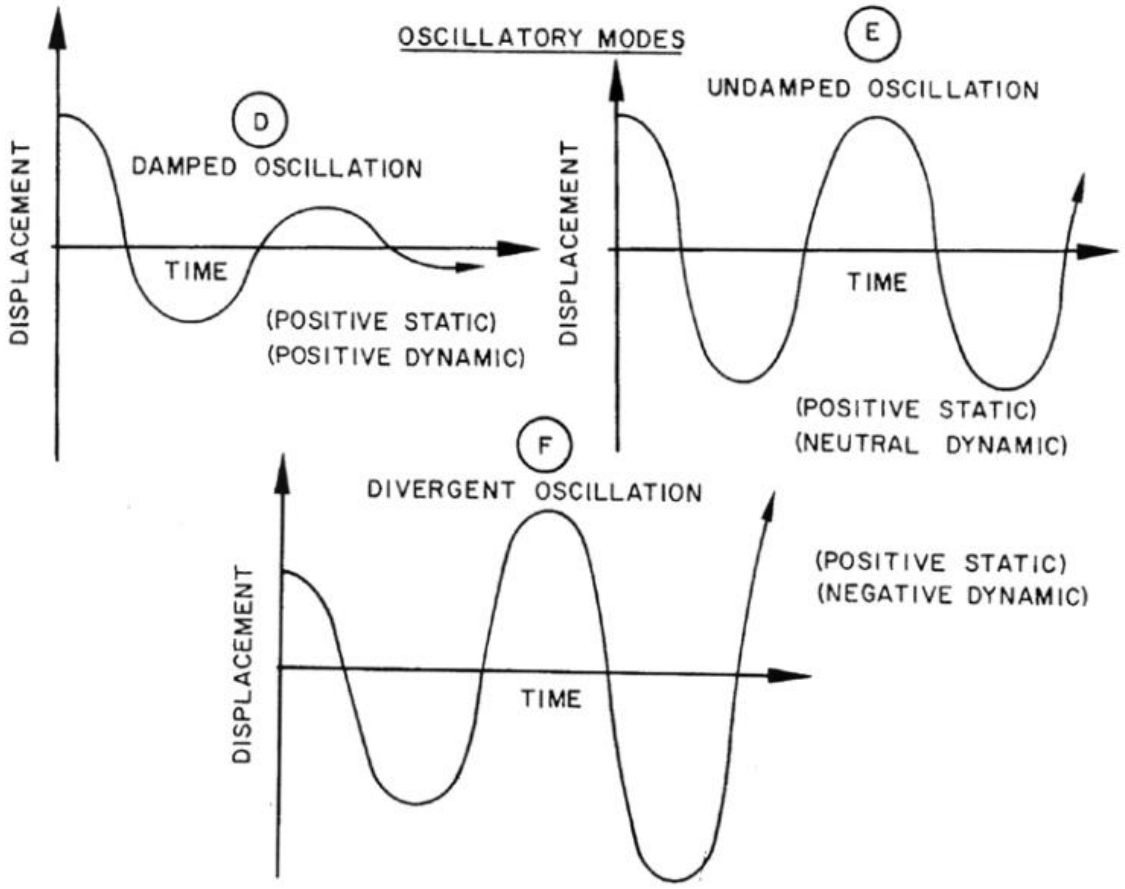

Figure 23. Example of Decaying, Steady, and Unstable Responses. Source: [53].

10. Base Drag Reduction

The aerodynamic design of the SUAVE is intended to achieve two goals, in the following order: first, to achieve a tight turn. The second goal is to maximize the effective range of the vehicle. This secondary objective is achieved through drag reduction, flight path modeling, and control optimization. Flight path modeling and control optimization can only be performed once the basic layout has been determined. Only then can more advanced analysis be conducted. While still in the preliminary design stages, drag reduction can be investigated.

In terms of drag, the significant contributors are the presented area, the surface area, and the base drag. The presented area is directly related to the missile body diameter, which is sized to accept the payload. The surface area is

a function of the vehicle diameter and length, and the number, shape, and size of fins. Greater knowledge of the payload would allow a review to see what trade-offs can be made in terms of packaging or component placement, and what reductions in drag would result. Any drag reductions can then be weighed against the impacts of the changes required to achieve them.

The base drag for this particular effort may be an area in which performance gains can be easily found. Base drag is due to the airflow over a insufficiently tapered reduction in diameter causing low pressure regions. These low pressure regions cause a force in the direction opposite that of flight (drag). A body which abruptly ends causes such low pressure regions. By tapering the aft of the body, some mitigation of the base drag can be obtained. The taper that can be included is limited however. The rocket nozzle provides one clear limitation to the extent of the taper; the loss of internal volume is another limit to the taper which can be achieved.

The SUAVE prototype vehicle is intended to allow for the use of a maximum of 102 mm (4 in) diameter rocket motors. Since the fore-body is sized for a 191 mm (7.5 in) internal diameter, there is a significant amount of unused volume around the rocket motor. It may be possible to transfer components to this area, at the cost of shifting the center of gravity further aft and negatively impacting the aerodynamic layout. This volume can also be eliminated. Either a boat-tail or transition can be used to trade unused volume for reduced drag. A boat-tail tapers the body to make the intended diameter coincident with the end of the rocket body. A transition includes a taper at some location before the end of the rocket body, so that the body consists of its large diameter, a transition to a smaller diameter, and the smaller diameter continues to the rocket nozzle. An additional benefit of a transition for the SUAVE design is that the reduction of body diameter at the tail allows for a greater semi-span within the span restrictions applied to the canards. This reduction could allow sufficient rear fin size and shape without exceeding the canard span restrictions, so that the

vehicle would provide a coherent packaging solution. Further investigation of the use of a transition section is therefore recommended.

Use of a boat-tail or transition will affect the airflow near and aft of these features. It is not expected that Missile Lab provides accurate values in the presence of such features. Therefore, further investigation regarding flow characteristics within the vehicle's intended mid-Mach flight regime is recommended should boat-tailing or a transition be employed.

D. PROPULSION

There are many different types of propulsion available for an air vehicle. The primary concerns for a tactical vehicle are minimum maintenance, rapid ignition, and minimum storage concerns. Solid fuel rocket motors offer large amounts of stored energy in a mechanically simple package with low storage requirements. To meet the COTS mandate, Cesaroni Pro-Series [54] solid rocket motors have been used. They have no moving parts and therefore minimal maintenance concerns, and can generally be transitioned from storage to usage with little additional preparation. The drawback of lack of reusability is not a concern for a tactical weapon, which is itself disposable.

Cesaroni rocket motors offer good performance and cost. These motors are intended for the hobbyist market and are therefore easy to use. There is a wide range of thrust profiles available and the SUAVE has a motor tube sized to allow a wide range of motors, so that the thrust profile of different motors can be substituted to meet evolving vehicle thrust needs. As a prototype vehicle intended for system development, this flexibility is extremely important.

E. RECOVERY

1. High Speed Deployment Background

The SUAVE is intended to be capable of autonomously controlled flight. Intended flight profiles include times during which the rocket will be in powered flight and with intended orientations other than perpendicular to the earth ("up").

In the event of failure or incorrect planning, there exists a definite possibility that the vehicle may erroneously adopt an incorrect heading, which will necessitate premature termination of the flight.

A particular launch saw the vehicle adopt a flight orientation parallel to the surface of the earth at high speed. As this is an unsafe condition for an unguided rocket, it was decided to activate the dual event system. Unfortunately this system was not sufficiently robust, and the parachutes became exposed to the very high speed airflow, which destroyed the parachutes. The rocket then fell to the ground with very little additional drag and suffered significant damage. Based on this experience, the subsequent system was designed to function in all foreseeable deployment conditions.

Based on the experience residing in the NPS Rocket Lab, the recovery system has designed to overcome practical problems. For general hobbyist rocket applications, deployment of the parachute is achieved by forcing the rocket to separate somewhere along its length. The sections are tied together and to the parachute as well. The parachute is ejected by the same mechanism which forces the sections apart, and unfurls in the airflow around it.

2. Deployment Concept

For the SUAVE prototype vehicle, it was chosen to employ a three “event” recovery sequence. Each event is the initiation of a stored energy component, which alters the configuration of the vehicle. This three event sequence was chosen in response to experience gained by the NPS Rocket Lab through similar development efforts conducted in support of the ME4704 course, and is intended to mitigate recovery system damage from a high-speed deployment event.

This deployment system’s conceptual functioning is as follows. Upon activation, the rocket is separated at a location near the middle of the rocket. This removes any aerodynamic stability of the resulting components and thereby increases drag. To increase the drag further, drag devices (streamers and/or drogue parachutes) are deployed during the initial event. This is intended to

rapidly bleed kinetic energy from the rocket, so that the main parachutes can be safely deployed. Initiation of this primary event is by redundant automatic controller at flight apogee with manual back-up.

Secondary events are the deployment of the parachutes from the fore and aft sections. Both the fore and aft systems function similarly, being initiated by redundant automatic controller at a user-defined altitude with manual back-up. Upon initiation, each section is separately separated into two parts connected by a shock chord. A parachute is tied to each shock chord; the shock chords being made of highly elastic para-aramid fibers, allowing them to stretch and avoid system damage as each pair of halves are arrested in their motion away from each other.

To avoid damage incurred after landing due to being dragged across the ground by desert winds, a parachute release mechanism is also employed. This release mechanism ruins the parachute's drag characteristics upon landing, so that wind gusts will not drag the rocket parts by the parachute across the ground. This system was found necessary after the prototype SUAVE suffered damage due to dragging by wind gusts.

A final consideration for the deployment system is pressure relief. As a rocket climbs into the air, the surrounding pressure decreases, whereas the internal pressure (unless vented) stays constant and therefore much higher if assembled on the ground. This pressure imbalance can force apart a rocket which is already designed to separate. One method of mitigation for this issue is the use of a mechanical restraint, such as shear pins, described in Chapter IV. Sec. F. Subsec. 2. Couplers. Another method is the use of vent holes, which allow the gradual equalization of pressure between an internal volume and the atmosphere. A recommended resource is provided for determining the size and quantity of pressure equalization holes [55]. Care must be taken when using these pressure equalization holes such that they do not significantly inhibit the function of the CO_2 system, as shown in Figure 24.

In the test shown in Figure 24, the deployment system did not separate the rocket sections. This was due to the CO_2 gas prematurely venting through the pressure equalization holes.

Figure 24. Separation Test

3. Parachute Deployment System

The vehicle separation points are fitted with couplers. The couplers connect the rocket sections with the intent of minimizing motion between rocket sections during flight, while still allowing separation under all expected normal flight conditions. Coupler design is covered in more detail in the Structure sub-heading.

TAC-9 parachutes (no longer advertised on their manufacturer's website) are employed in the prototype SUAVE. These parachutes are well-sized to the application, are durable, and use only 4 connecting cords which greatly simplifies pre-flight preparation. The TAC-9 parachutes were formerly distributed by Giant Leap Rocketry [56].

Separation is achieved via a CO_2 system, also referred to as a cold gas system. The traditional method of deploying parachutes for hobbyist rockets is by

means of black powder charges initiated by 9V battery fired igniters (called “e-matches”). Doing so causes the deposition of large amounts of corrosive black powder combustion residue. These deposits necessitate significant post-launch component cleaning, and mandate increased handling of explosive-classed materials. In addition, black powder functionality is suspect at higher altitude due to the lower ambient pressure inhibiting combustion. For these reasons, it was decided to use a CO_2 system. A review of available systems identified the CD3 HPR Kit [57], which provides a lightweight and affordable solution for CO_2-based deployment. This system uses an e-match to ignite a small amount of black powder in a piston. The piston is propelled forward to pierce the rupture membrane of a common CO_2 cylinder. The CO_2 gas is vented into the rocket’s parachute bay, where it pushes against the parachute and simultaneously forces the female portion of the coupler away from the male. The parachute is thereby exposed to the airflow, and is pulled away and unraveled by the airflow, without relying on any initial impetus from the compressed gas. Three of these CO_2 systems are used on the prototype SUAVE; one for each event. Each CO_2 system contains a single black powder charge and cartridge. Therefore, the CO_2 system does not include any redundancy, and so care in design must be exercised to ensure that once initiated, separation will occur correctly and not be impeded by undue friction or forces from unexpected flight conditions.

Selection of the CO_2 cartridge must be done to meet the expected size of the volume which will be pressurized. A sizing chart is available [57].

Testing of the CO_2 system was carried out to ensure that the system would work in this application. The first test used the propulsion and recovery sections coupled together, and placed at a low angle relative to the ground, supported by the rear fins and a point just aft of the recovery section, so that the weight of the recovery section was borne entirely by the coupler for maximum friction, as seen in Figure 24. As mentioned earlier, the first test failed due to the pressure equalization holes allowing venting of the high-pressure gas before the components were able to separate. Filling these holes and relying on the shear

pins to restrain the components in the face of external/internal pressure imbalances solved these problems.

Control of the separation events was by automated Perfect Flite Stratologger [58] control boards, with a Missile Works WRC+ Remote Control System [59] serving as manual back-up in case of failure of the automatic system. The Stratologgers are programmable both via interfacing with a computer, and directly with the control board itself via buttons with user information output as a sequence of audible beeps. A concern regarding the use of the Perfect Flite Stratologgers is the available channels. One channel is set to send a 9V battery signal upon reaching flight apogee, and the other channel is set to send its 9V battery signal once a user-set altitude is reached during descent. This means that this controller will not be appropriate for use on any flight paths that include sections of flight carried out after the vehicle has begun descending. There are many other deployment control systems available. It is strongly recommended to determine the deployment requirements for future development, review the current COTS systems, and acquire the most appropriate controller. A barometer is used to determine altitude, and this altitude data as a function of time is stored by the Stratologger and can be accessed for post-flight analysis. The barometer reads local ambient pressure, and so pressure-equalization holes must be drilled in the rocket body near the control boards. Recommendations regarding the pressure equalization holes (number, size) are available from in the Stratologger installation manual [60].

The Missile Works WRC+ system is a radio-operated initiation system employed as a manual back-up. Upon receipt of a signal from the user's remote control, current from the board's 9V battery source will be directed to the terminal set related to the button the user pressed. These boards offer four different user-initiated channels, and several additional features which have not yet been required for the project. The boards are physically relatively large, but have worked well in the experience gathered by the NPS Rocket Lab.

In order to advantageously orient the missile halves after primary separation, drag mechanisms are deployed during this event. The goal of these drag mechanisms is primarily to increase the drag on the component so as to slow the component in the event of separation at high speed, and to both minimize tumbling which may cause additional forces at the un-released couplers which could impede additional separation events and to orient the components in hopes of aiding the separation. It is thought that if the component's orientation to the freestream is somewhat controlled, then the separation will be more likely to succeed.

To achieve these ends, a streamer is attached to the rear of the fore section. This streamer has successfully unfurled in all tests. The fore section parachute has deployed reliably in every test. It is recommended that the fore section's streamer is retained until such time as a solid rationale for change is found.

The aft section uses a drogue parachute, which is a small parachute intended "to be deployed from a rapidly moving object in order to slow the object, to provide control and stability, or as a pilot parachute to deploy a larger parachute" [61]. The drogue replaces the earlier streamer, as discussed in Chapter V. Sec. A. 3 June 2017 Launch. The drogue has a tendency to foul in the rear fins. This can be avoided by use of a sufficiently short lead, but it is not known if this will cause the drogue to get caught against the body by the airflow. Other methods, such as forced drogue ejection, should also be considered.

Ground dragging is avoided by means of a FXC Parachute Release mechanism [62]. These mechanisms begin to arm once a tension load is attached to the shackles. The tension pulls internal components away from each other while slowed by a hydraulic damper. Once the components have been sufficiently displaced, the system is armed. Removal of the load will cause the release of one of the shackles. The smallest of the available FXC systems is employed [63], which is intended for payloads weighing in excess of 22.7 kg (50 lbs). As the payload does not meet this weight, further testing was carried out by

2017 Q2 ME4704 course members which determined that the system correctly arms in 9.5 seconds [64]. The FXC mechanism is plumbed into the parachute connection between the base of the parachute line combination point and the shock cord. A leader is attached from the shock cord to the parachute so that the parachute will not get lost once disconnected by the FXC parachute release mechanism.

Parallel to design of the FXC system, a back-up strategy regarding canard damage was also designed. The concept employed is to introduce a point of expected failure in the event of ground dragging. This can be achieved by allowing the canard fins to break away from the body so as not to be further damaged or cause damage to the actuator mechanism. As the canard fin holders are attached to the actuator shafts by two screws and two dowel pins, careful sizing of the screws allows the fastener strength to exceed flight loads, but to be overmatched by dragging loads. It is reasoned that as the canards are damaged by dragging but not flight loads, then the dragging loads exceed the flight loads, and surpassing the flight load threshold is sufficient to achieve the intent. Reviewing the available screws, and calculating expected loads at the screws, it is found that use of brass screws provides the desired characteristics by exceeding the expected flight loads by 7.98%.

F. WEIGHT

1. Structure

The basic structure of the vehicle is a tube, which acts as the main load-bearing component. To this tube are affixed all the parts necessary for the rocket to perform its function. The tube chosen is a fiberglass wrapped phenolic tube of 191 mm (7.5 in) internal diameter from Public Missiles [65]. Wall thickness is a nominal 3.2 mm (0.125 in), and the linear density as measured on samples received at the NPS Rocket Lab is 1.505 kg (3.318 lbs) per 685.8 mm (27 in) of length 2.2 g/mm (0.123 lbs/in) length. This tubing has not been tested for material properties other than linear density.

2. Couplers

Couplers provide the interface between sections. These are intended to minimize unintended motion between sections, while easing the ability of the sections to separate when the deployment system is initiated. The most difficult type of unintended motion to counter is loss of collinearity between connecting sections, as seen in Figure 25. Currently each set of couplers are different due to design evolution. As the design has evolved, it was found that increasing engagement length is the most practical method of minimizing angular deflection and maintain collinearity between the center axes of coupled sections.

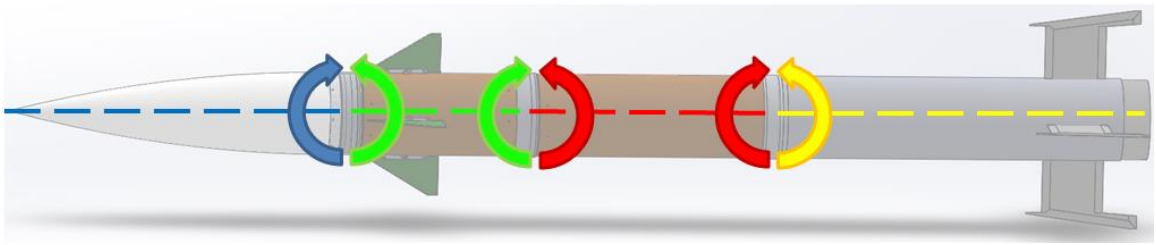

Figure 25. Undesirable Motion

The first set of couplers is located between the nose and control sections. The intent of this design is to use metal in order to allow better diameter control, so that only a short engagement length is required for a minimum amount of bending of the longitudinal axis. This first set of couplers relies on the geometry shown in Figure 26 to resist bending of the longitudinal axis. A dual diameter design is used, each diameter having a separate bearing surface approximately 3/8 inches in length. By using dual diameters, the coupler has only to disengage the bearing surface by moving axially the 9.5 mm (3/8 in) before discovering a 3.2 mm (1/8 in) diametral clearance. When male and female are mated, diametral clearance is targeted at 0.051 mm (0.002 in), though manufacturing inaccuracy, wear, and temperature differentials all work to alter this value. Testing the play in the coupler fit for both the short metallic and long phenolic coupler types with a static bench test intended to discover the effective

accumulation of clearances in the assemblies provided the information in Figures 26 and 27. Because of aluminum components' tendency to gall when made to slide across each other, the use of some form of grease is strongly recommended when employing these couplers. High pressure machine greases are recommended, however anything that provides a thin fluid film while under pressure is applicable. For these reasons, it is recommended to employ the cheaper sliding fit phenolic couplers in future work on the vehicle.

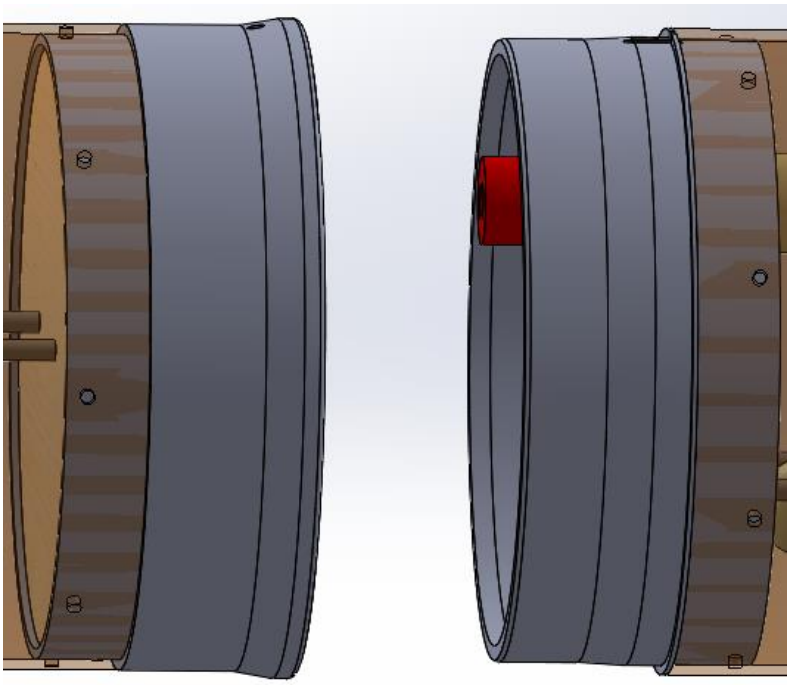

Figure 26. Aluminum Coupler with Tight Diametral Tolerance

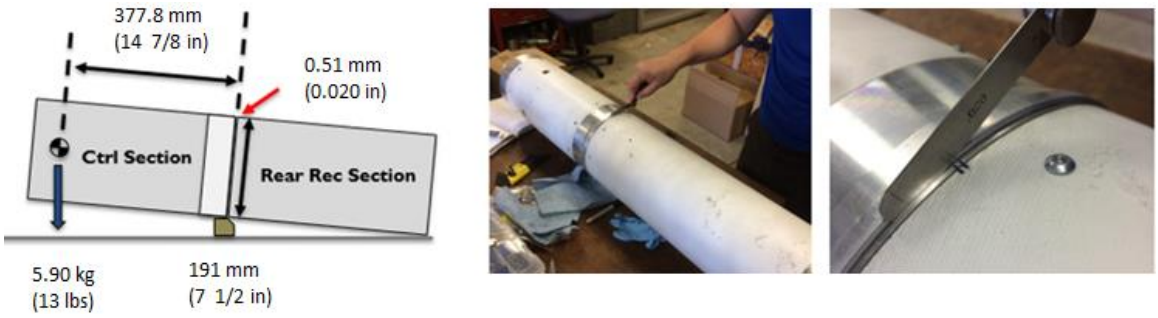

Figure 27. Bending Play in Short Length Metallic Coupler

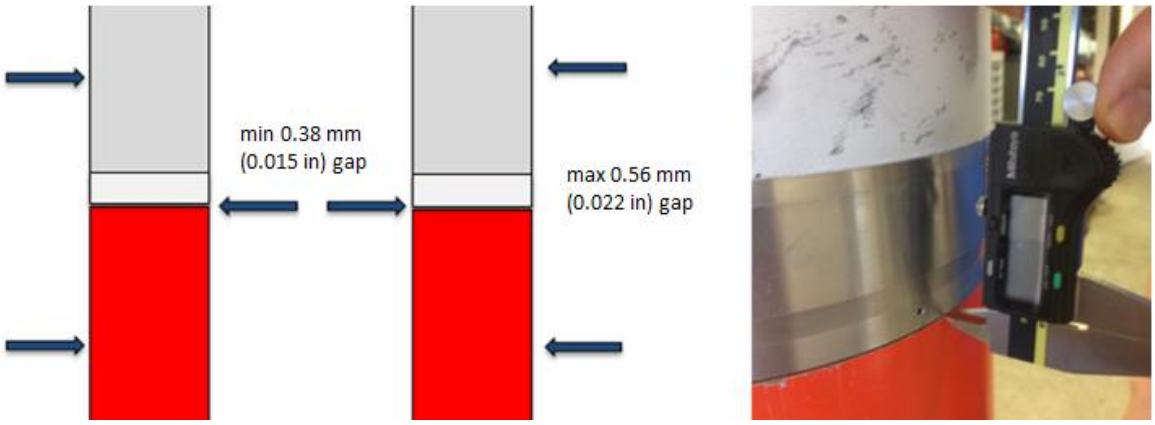

Figure 28. Bending Play in Long Length Phenolic Coupler

The second set of couplers is located between the control and recovery sections. This design is a modified version of the first set, incorporating an anti-rotation device in the form of a standard machine shaft key. Use of canards to counter vehicle roll causes forces that are opposed by the tail fins; this induces a torque transmitted through the vehicle, and which the coupler must likewise transfer without allowing rotation at its connection. Mild steel was used for the key as it bears on aluminum and thus is stronger than the surrounding material. Sizing was performed by stress analysis to avoid the compressive failure of the aluminum upon which the key bears. Assuming each of the four fins would generate 30 lbf modeled as a point load at the mid-semi-span, this can be translated into a pressure borne by the aluminum face in contact with the key. Doing so, it was found that the key requires a bearing surface measuring 11.125 mm (0.438 in) by 0.381 mm (0.015 in); this last dimension being increased to 0.889 mm (0.035 in) to provide a safety factor. Width of the key was taken as stock size, and so the key is a rectangular prism of 11.125 mm (0.438 in) by 1.778 mm (0.07 in) by 4.763 mm (0.1875 in). Key retention to the male coupler is achieved by means of a screw inserted through the interior of the coupler to the screw threads in the key. A chip clearance hole was required in the female coupler for clearance of metal chips created during the manufacturing process. This keyway is seen in Figure 29. As a note of future reference, this internal keyway was cut by using a lathe as a shaper tool.

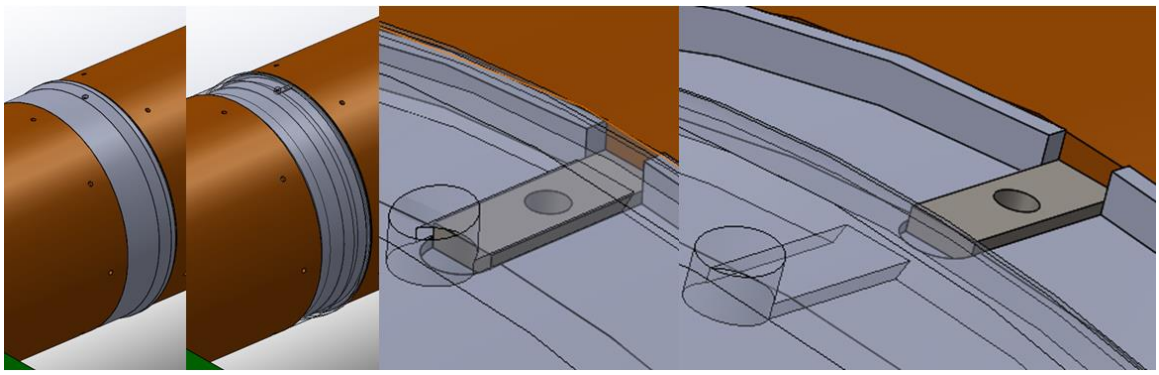

Figure 29. Coupler Keyway Detail

The third set of couplers is located between the recovery and propulsion sections. This design is a modification of a coupler design commonly employed by amateur rocket enthusiasts, which does not rely on a close diametral fit. This is an advantage because holding a tight diametral tolerance on a thin-walled structure is difficult for manufacturing and becomes significantly more difficult as the length increases. That design was very similar to the standard hobbyist practice of concentric sliding tubes, but with structural reinforcement in the form of an additional coupler inserted inside the coupler tube and bonded together with epoxy. Additionally, a pair of threaded rods run parallel to the longitudinal axis and are loaded in tension to pull a pair of plywood bulkheads against the inner coupler tube. This design provides a 165.1 mm (6.5 in) coupler axial engagement length. An aluminum ring was added which caps the end of the female coupler, providing an impact resistant lip against the shock cord which has a tendency to be driven violently against the inside of the tube during parachute deployment and landings, as well as providing a good bearing surface for the rear coupler anti-rotation device. This rear anti-rotation device is again a single key, but in this case extends radially from the missile axis the entire thickness of the lip. The phenolic type coupler is seen in Figure 30. It is affixed with epoxy-type glue to the male coupler; this method allowing gluing while assembled and therefore excellent alignment.

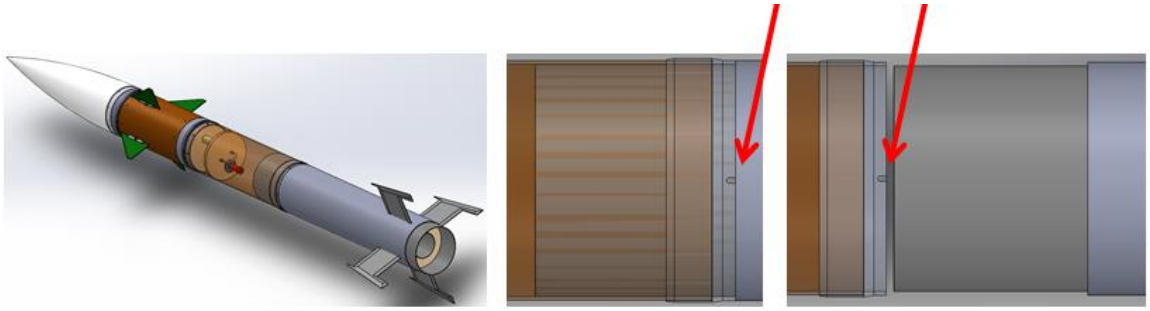

Figure 30. Long Length Phenolic Coupler

All couplers are kept from separating before initiation by means of shear pins. These are small pieces of material which are intended to be sheared apart by the opening couplers due to the pressures generated by the deployment system. Currently employed are six pins per coupler set, each pin being a 2–56 nylon pan head screw; the head allowing for ease of removal in the case of the couplers requiring disassembly after pin insertion. The nylon threads easily deform during insertion, conforming to the diameter they meet.

G. ELECTRONICS

1. Requirements

The intended SUAVE requires a method of executing GNC functions, and a data-link to receive target updates from the ground-based sensor. Payload deployment/initiation timing is to be related to the SUAVE's proximity to the target location as determined by the GNC system. On board processing is intended to be performed by whichever current-generation small computer is cost-effective for the application. Recent reduction in processor cost is a major technological change which the SUAVE is intended to leverage. Battery technology has likewise allowed small and low-cost batteries to provide sufficient power to run all expected on board systems for a period longer than a single flight requires. Note that the deployment controllers are described under the Recovery section.

2. Battery

Once development is more nearly complete, the SUAVE will require a battery sufficient to provide power throughout the expected flight duration. During the prototype phase, the SUAVE carries a larger battery which provides power for multiple flights. The additional weight is counted toward the expected payload. A 8000 mAh battery was installed to alleviate issues with loss of power for the servos due to long pre-launch waiting times.

The recovery system uses a collection of 9V batteries for its power. Power for the recovery system is independent of the rest of the control system.

3. Processor

To achieve the GNC functions, a processor is required. The processor accepts target location inputs and converts these into control signals for the actuators, specifically in the form of Pulse Width Modulation signals which are the correct format for the selected actuators. SUAVE work covered in this thesis did not focus on the design of the GNC system.

Currently the SUAVE employs an Arduino Due microcontroller [66]. This processor allows the execution of simple instruction sets, which must each be programmed using the Arduino Software (IDE). Arduino Due microcontrollers offer low weight, cost, and power consumption, but have a relatively limited memory available for their command set. Libraries are available [67] with pre-compiled code which can be modified to suit a specific user requirement. Many tutorials for writing codes for Arduino microcontrollers are available online. Arduino code employed on the SUAVE prototype is included in the appendix. The INS used is a BNO055 Intelligent 9-axis absolute orientation sensor [68].

As per discussion with Prof Dobrokhodov [69], the recommended processor for implementation of a GNC system is the Hardkernel ODROID-C2 [70] with the BNO055. Using the model without fan is recommended [69], so as to avoid issues that the fan will face when subjected to accelerations during flight. The ODROID is a single-board computer [71], making it more sophisticated than an Arduino

microcontroller. This increased sophistication means that the ODROID has greater capability, but is also more complicated to learn to use. ODROIDs run an operating system (often Linux), and this operating system can run other user-input computer programs. In order to achieve the best results regarding implementing a GNC system on a missile, it was recommended to run Robot Operating System (ROS) in Linux on an ODROID [69]. ROS is "…a set of software libraries and tools that help you build robot applications. From drivers to state-of-the-art algorithms, and with powerful developer tools, ROS has what you need for your next robotics project. And it's all open source" [72]. This is advantageous because it allows the use of many pre-existing pieces of software, which can be modified as (or if) required by the user to achieve the desired results. This is a huge savings in labor when compared to the Herculean task of writing each and all the commands and subroutines that a GNC system requires. As the goal of this project is to minimize costs (including developmental) by leveraging emerging technology, the use of ROS fits the project intent and mandate.

The ODROID requires a constant supply of 5V power, with power consumption ranging from 0.5 to 2 Amps [73]. As the SUAVE prototype uses on board batteries as power supplies, whose voltage drops as the battery discharges, a means of power conversion is required. This is achieved by using a Buck Boost Converter [74], which is "a type of DC-to-DC converter that has an output voltage magnitude that is either greater than or less than the input voltage magnitude" [75]. This means that power fed into the buck-boost converter will be output at the desired voltage, so long as the input power is within the accepted range (5 to 25 V) of the buck-boost converter.

V. TEST CAMPAIGN

All launches were conducted at the Friends of Amateur Rocketry site in the Mojave Desert. Weather at this location averages 39 deg C in the summer, and an average low of -3 deg C in the winter. Humidity is low, and there is a large amount of sunny days, making this a good location climatically for rocket launches.

A. 3 JUNE 2017 LAUNCH

Launch goals for the first flight of the canard controlled SUAVE were to verify the recovery system and anti-roll systems. A single launch was conducted. The recovery achieved the goal, as the vehicle was undamaged during the landing. The anti-roll system however was found to not work, and required further design effort.

Since the goal of the launch was to verify that the recovery system itself allowed the rocket to return to the earth undamaged, this system can be claimed as successful. However, not all parts of the deployment concept functioned as intended, and the upper half of the vehicle was damaged by being dragged through the desert after landing.

The deployment system is intended to use streamers to orient the fore and aft halves after separation. The aft half is intended to fall fins-first. To do so we start with a first-order approximation and ignoring the body force, there must be greater drag at the end opposite the fins, similar to Figure 31. It was seen that the aft end fell forward first and not aft first as intended. The streamer became pushed against the side of the vehicle as it fell. Despite the undesirable orientation, the parachute was found to deploy correctly. This successful deployment was very encouraging given that the vehicle began to fall very quickly (approximately 30 m/s). Plans for improvement of the orientation after separation involved an extended lead on the streamer with the intent of keeping the streamer from laying against the side of the body. A free body diagram of the

aft half in cross-wind flow is provided in Figure 31, showing the drag imbalance required to correctly orient the vehicle.

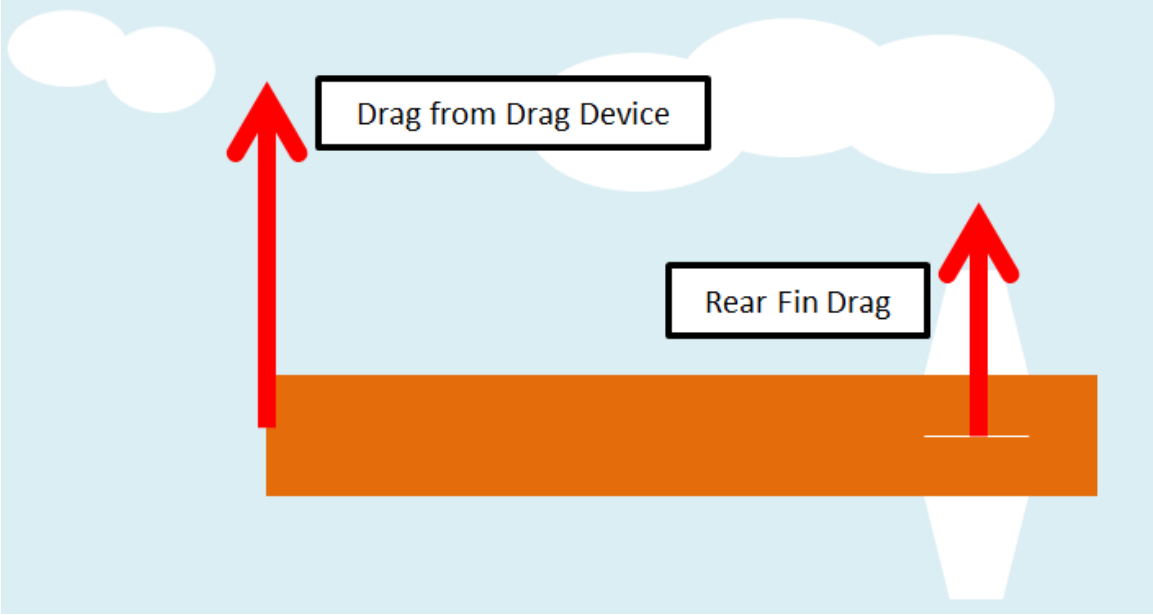

Figure 31. Aft Half Comparison of Front and Back Forces

Anti-roll was to be achieved by using the canards to provide torque counter to any detected roll. The defect in this system was that the shear pins in the couplers were insufficient to withstand the loads imposed by the anti-roll system, and so the control section was able to rotate relative to the propulsion section. Video footage reveals that the recovery section would rotate with either the control section or the propulsion section intermittently. To solve this issue, anti-rotation keys were built into the middle and aft couplers.

The vehicle was able to land correctly and without damage, but a wind gust after landing caught the control section parachute and dragged the section through the desert. This caused functional damage to the fin holders, which were made from formed thin gauge mild sheet steel. One of the gears was also found to have skipped some teeth, thus ruining the alignment. To solve this issue, a

parachute release mechanism was researched in order to deflate the parachute after landing on future flights.

B. 2 SEPTEMBER 2017 LAUNCH

Launch goals for the second flight of the SUAVE prototype involved data logging, an updated anti-roll system, a commanded pitch of the missile to demonstrate controllability, solve the dragging damage issue, and perform a minimum of two launches during this launch day. These goals were partially met. Overall, the missile was able to attain altitude, execute a pitch command, and recover without damage. This flight was the culmination of the 2017 Q4 ME4704 course, and much of the work was conducted by the members of that course.

Data logging was intended to verify the accuracy of the inertial navigation system (INS) on the Arduino, using a Lord Microstrain [76] as a reference. In order to log information from the Lord system, a Raspberry Pi 3 [77] was used. Unfortunately, although compatibility of the two systems was advertised by Lord, it was found that the two components required significant development beyond the scope of the course to function properly. It was decided that the Lord system would not be flown in the near future due to the compatibility issues with the Raspberry Pi 3. Reviewing the Lord to ODROID compatibility is recommended for future efforts to verify INS accuracy.

Anti-roll achieved the design intent during the straight climb, but not during the subsequent pitch maneuver. The intent of the anti-roll is to limit body roll. As can be seen in the photos from the launch, the roll angle of the body with respect to a reference (taken as the shadow, which is deemed sufficiently precise for this application) changed during the vertical ascent. Anti-roll design must include quantifiable limits to allowable body roll. The body roll during ascent can be roughly measured by direct analysis of the flight camera footage, shown in Figure 32. From these photos, it can be seen that the shadow was at an angle of 92 degrees from a line drawn parallel to the video’s vertical reference. This angle decreased during ascent to a minimum of 69 deg, then increased to 99 deg

before beginning to pitch. This change can be expressed in several ways; for example, either as angular displacement from the initial reference, or as a bilateral range from the midpoint of the extremes. Total range in angle was 30 deg. Assuming a +/-2 deg measurement error, the total range is 26 deg, with a maximum deviation from initial position of 19 degrees. With the +/-2 deg assumption in measurement error, the system functioned as intended, by meeting the specification of limiting change from initial roll angle to less than 20 deg.

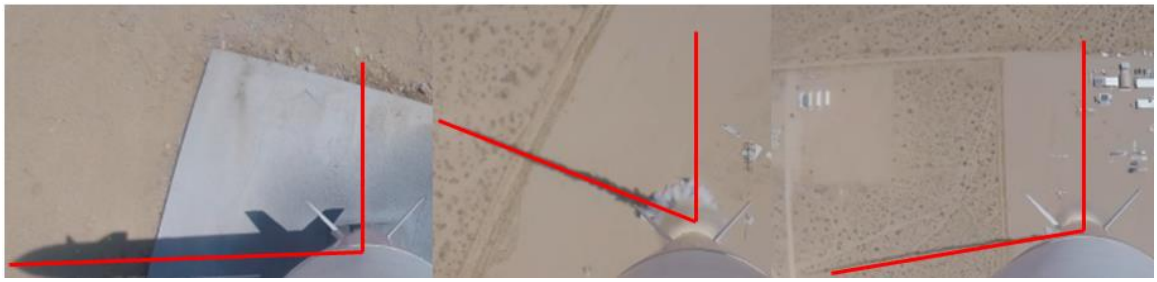

Figure 32. Roll During Vertical Ascent of 2 September 2017 Flight

Pitch command performance is deemed acceptable at first review. The objective was to have the vehicle display the ability to pitch over, and this is what is visible in the video from the launch. Unfortunately during this maneuver, the roll control system did not succeed at limiting roll to less than 20 deg displacement from initial angle, and therefore the commanded anti-roll fin deflections will need to be increased. During the pitching maneuver, two of the four canard fins are given pitch-inducing deflections, while the remaining two are left for anti-roll. A review of the impact of It is recommended for future work to establish target pitch rates over the desired range of flight speeds, and to define and validate a method by which to measure the pitch rate. It is strongly suggested to validate the INS data which the control system responses are based on.

Dragging damage was intended to be mitigated by the use of the FXC Parachute Release Mechanism. Winds on launch day were quite low, and so the control section was not subject to any dragging after landing. Instead, the control section settled upright on the desert floor and the parachute gently settled all about it. On inspection of the FXC mechanism, it was seen that it had functioned as expected, in that the retaining mechanism had opened, so that the parachute connection should have been released if it had not settled so gently. Therefore, although the system has yet to be fully tested, it is expected to work satisfactorily in a landing where ground-level wind is present.

Only one SUAVE launch was performed on 2 September 2017. It is believed that the turn time (which is the time required to recover and ready the SUAVE prototype between launches) was too long. The main factors identified were continued issues with electronics access, CO_2 system consumables replacement, parachute preparation, and motor preparation.

Electronics access is required to perform 9V battery load tests, the LiPo battery voltage test, replacement of data storage media as appropriate, control system interface, and turning on/off the recovery controls, the control system, and the servos. For this flight, an access panel had been installed. Behind this panel were switches for the three recovery control boards, the servos, the Arduino controller, and the Raspberry Pi 3-based data logging set up. Unfortunately a small power on/off button on the Raspberry Pi 3 remained inaccessible after the build-up, and so the switch panel did not allow access to all necessary controls. Location of the switch panel unfortunately also coincided with the location of the rail guide buttons; and so the switch panel was held against the launch rail when the missile was loaded onto the rail. This was partly mitigated by the installation of a switch panel door that is entirely removable; however, the overall functionality of the switch panel was deemed to be poor. Suggestions include ensuring all required functions are accessible, and that the door is located opposite the rail-mounting side of the vehicle.

CO_2 system consumables replacement is a long process. Each of the three CO_2 systems use a single CO_2 cylinder and three consumable e-matches in a holder with position for two e-matches. The e-match holder is being replaced with new holders, with positions for three e-matches each, manufactured in sufficient quantity so as to allow the e-match holders to be assembled before launch day. Each e-match must be wired to a recovery control board. By ensuring a terminal block is located beside each CO_2 system, past wiring accessibility problems will be avoided. Not addressed is accessibility of the CO_2 cylinders; it is recommended that accessibility be eased in order to further reduce turn time.

To prepare the vehicle for launch, the parachutes must be cleaned, folded, and packed. There are currently no recommended methods for speeding this process.

Motors require some amount of preparation and installation between flights. There are currently no recommended methods for speeding this process. It is recommended to time all activities involved in recovery and preparation for flight in order to identify all activities, length of activities, and required skill sets, in order to minimize time spent sweating in the desert heat.

C. 17 NOVEMBER 2017 LAUNCH

Launch goals for the third SUAVE prototype flight involved validating aerodynamic predictions and decreased turn time. Through use of the Missile Lab software, an aerodynamic design which indicated the potential of attainment of a 15 deg body angle of attack had been created. Implementation of this design was through building a new propulsion section for the rocket which incorporated a new fin planform. The turn time was to be further reduced by the use of new e-match holders and wiring terminals.

Predictions of the SUAVE's performance with varying rear fin planforms indicated that the required shape include a very long and narrow delta, which was overhung from the attached zero sweep section both front and rear in an

attempt to maintain fin strength. This caused a narrow section of the delta to project further forward than the rest of the fin, which caused issues with the recovery equipment.

Main separation was initiated with the vehicle approximately horizontal and moving quickly. The halves were not thrown sufficiently clear for the important drag inducing components, meant to slow the vehicle given recovery under these conditions, to avoid the fins. The front half's streamer was torn by the rear fin, which did not seem to greatly diminish its performance. The rear half had been equipped with a drogue parachute. This was attached by means of a lead; the length being a choice between a long lead with the possibility of getting caught on the rear fins, or a short lead which could not reach the rear fins but left the possibility of the drogue being pushed against the rocket body by aerodynamic forces. This last had happened to the streamer in the previous launch, and so a long lead was chosen. Unfortunately this allowed the drogue to become entangle about a fin (see Figure 33), which led to the drogue not functioning and later lost when the rear separated and the lead was severed.

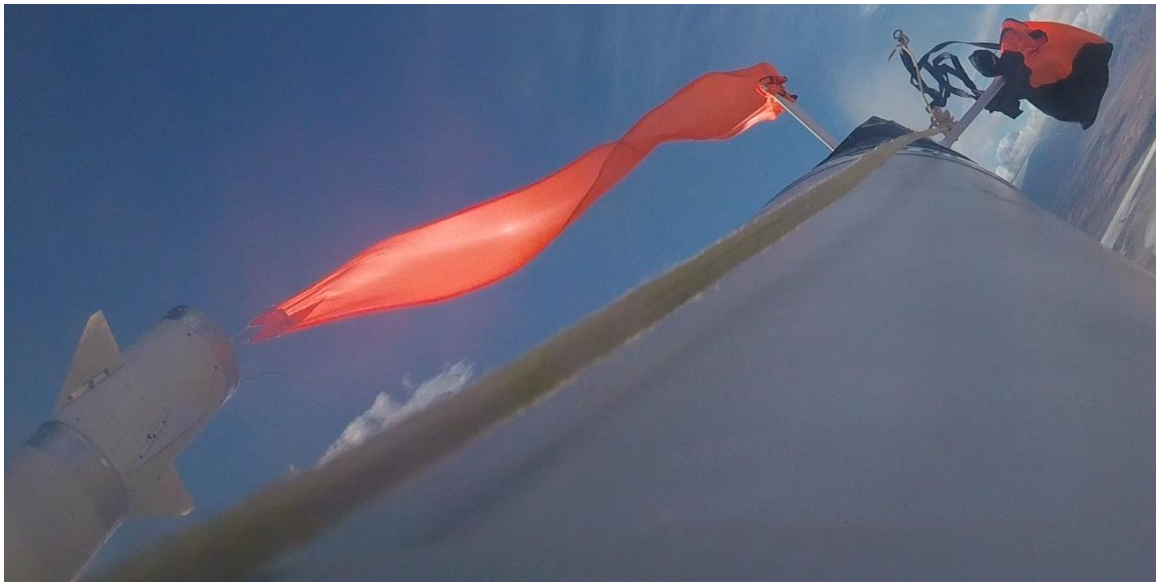

Figure 33. Drag Equipment / Rear Fin Interaction

Without the drogue's drag to slow the vehicle, the parachute was also lost due to excessive speed. Review of the damage suggests that the propulsion section, being the heavier of the halves connected to the parachute by a longer lead, caused abrupt impact-type loading once its shock cord was pulled tight. See Figure 34. Although badly damaged, the parachute was still sufficient such that the aft sections did not suffer significant damage upon landing.

Figure 34. Parachute Failure; Inset is the Video Frame Prior to the Frame Shown Large

It is recommended that for future flights, the fins be altered to allow the recovery equipment to slide off and away during collision, or that the recovery system be modified such that the drag devices are sufficiently ejected to avoid collision with the fins. Alteration of fin geometry will reduce the desired aerodynamic performance predictions; but it is felt that this is acceptable until the vehicle is proved to perform more basic tasks such as GNC, recovery without damage, and short turn times more reliably.

It was desired for the vehicle to perform multiple launches during a single launch day. To achieve this, new e-match holders were created with capacity for three vice two e-matches, which removed the requirement to modify the e-matches themselves, and was an improvement. Sufficient holders were created so that the holders can be pre-loaded prior to launch day. Electrical connections were somewhat improved with the addition of a terminal block for the forward parachute deployment. It is recommended however to review the rear electrical connections and CO_2 cylinder access, as changing components at these locations continues to be slow. The electronics bay was reorganized, with a new access panel unobstructed by the launch rail. This electronics bay allows increased access to components, but it is recommended to rewire the cannon plug, add 9V load test terminals, and wire in deployment LEDs and any electrical connections required by the particular control boards installed, to take full advantage of the electronics reorganization.

Throughout the flight, data was logged by the Arduino. It was hoped that this data set would provide an accurate set of flight velocities, acceleration, and rotation rates for post-flight review. Upon analyzing the data, it was found that the data was not sufficiently accurate to provide an accurate review of the flight. This raised concerns more important than post-processing techniques, as the data was intended to allow the vehicle to navigate through its flight. If the data is insufficient to describe the vehicle’s motion with a minimum of post-processing, then the data would not be sufficient to guide the vehicle during its flight.

Therefore, the question regarding post-flight data review is not how to post-process, but rather if the data is sufficiently accurate to guide flight.

Navigation is envisaged to be achieved through dead-reckoning. For this to happen, the vehicle must be relate the integrated roll rates with the double integrated accelerations in order to have position data in an Earth-fixed reference frame. Two numerical integration methods were attempted on the roll rate data; the first being a trapezoidal method, and the second being a 3-Point Newton-Coates method. The results of neither of these methods matched the flight video well.

Logged data shows a large deviation from data point to data point, which is obvious on a plot of the acceleration data such as Figure 35. Logged data time steps are also not consistent. Time steps vary from 22 ms to 40 ms, which is a change of 81% in data sampling rate, in some cases between individual data points. There is no discernible pattern to the variation in sample times. It is suspected that these changes are due to the nature of the code which includes the data logging and/or the data logging hardware. The code includes a loop within which flight commands are executed dependent on “if” statements and data is logged. Due to the “if” statements, the time required for each loop is inconsistent, and therefore the command to write data will occur at different intervals. Writing data onto an SD card on the Arduino shield requires some time, and it is unknown if this affects the write interval. Data is provided by the BNO055 INS sensor, and differences in the time at which data is made available by this sensor, and when the Arduino reads the available data are unknown. It is recommended that all aspects required by the dead reckoning navigation system be reviewed for rate compatibility.

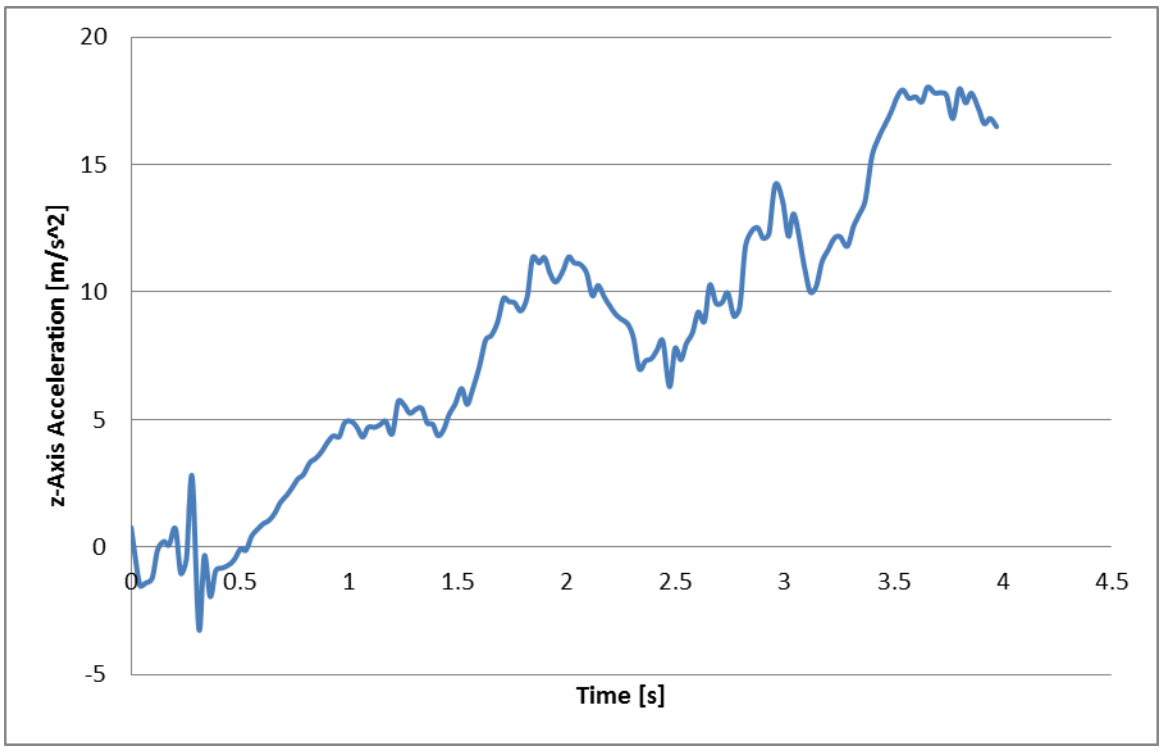

Figure 35. 17 November 2017 Flight Data Sample

Data obtained from this flight could be processed to yield an approximation of the trajectory, velocity, and roll rates, however this data would not greatly aid further development. Post processing techniques would not lend themselves to near-real time operation, and would not be implementable or appropriate on the flight vehicle. It is recommended to focus on further refining the flight controller, so that elaborate post processing of flight data is not required.

THIS PAGE INTENTIONALLY LEFT BLANK

VI. COST INFORMATION

Compiling the cost of the COTS components used in the prototype that are envisaged to be part of the final product, the total cost is approximately $4300 USD as of late 2017. This is a rough estimate, as certain components were manufactured in house, no volume purchase was applied, and labor of manufacture is not included. Some of these factors would drive the price up, and others would drive the price down. It is recommended that this figure be used with those caveats just identified, to guide further development and review of usefulness of the SUAVE projectile in comparison to other systems.

The implication of this rough cost is that the eventual payload should be capable of defeating no fewer than four opponents. This figure is a useful performance target for future work on payload definition.

THIS PAGE INTENTIONALLY LEFT BLANK

VII. CONCLUSIONS

A. PROGRAMS AND PROJECTS

The difference between a program and a project lies in the scope of the work required. A guided missile is a collection of systems, each of which is often the focus of a specialty field. The approach taken in this thesis was to work on every system, as required, to further define a missile-based swarm interceptor from a rough concept toward a vehicle whose performance could be measured. This allowed the author to become involved in a broad range of missile design topics, which point of view is generally reserved for a missile system's chief designer. An alternative and more common approach is to take a specialist's role, and with a narrowed focus, attempt to refine and advance a small area of the missile design. By acting as a specialist, more improvement can be made to a limited number of systems. By taking the position of chief designer to this system, the author was able to engage in a unique experience, as the needs of different systems had to be juggled so that the vehicle requirements could best be met with the available resources.

For future development, it is recommended that at the very beginning of a student's work it be decided as to how a project is to proceed. If a particular aspect of the vehicle requires advancement and significant work, such as both the payload and control systems, it is recommended that a specialist's role within the overall missile design framework be adopted until the system is sufficiently advanced. In so doing, individual subsystems will receive the focus that is required in order to progress.

B. SUMMARY

Activities in support of this thesis focused on the completion of a low-cost prototype anti-swarm missile vehicle. The culmination of these activities was a canard controlled missile-type flight vehicle with solid rocket motor propulsion, designed to meet the target performance metrics. To meet the requirements of a

prototyping vehicle, an effective recovery system was designed and integrated into the vehicle design. To generate the target performance metrics, a theoretical design of the expected threat was used in conjunction with the intended system operation concept. This allowed identifying not just the cost and kinematic performance metrics, but also the definition of the overall mission plan, and two flight plans that are instrumental in defining the boundaries of the performance envelope. With the system requirements in mind, the vehicle's subsystems were created to collectively meet these targets. To this end and with assumptions regarding the final payload, the vehicle's propulsion, aerodynamics, control, and recovery subsystems were designed with cost limitations in mind. This created a vehicle comprised of configurable sections, which allows system flexibility to support further development.

VIII. FUTURE WORK

> Engineering design is the process of devising a system, component, or process to meet desired needs. It is a decision-making process (often iterative), in which the basic science and mathematics and engineering sciences are applied to convert resources optimally to meet a stated objective. Among the fundamental elements of the design process are the establishment of objectives and criteria, synthesis, analysis, construction, testing and evaluation. [78]

Using [78] as guidance and following Ulrich's Generic Design Process [34], which provides an approach applicable to the design of any system, there is a clear sequence. The sequence develops and then refines a concept, which is a lengthy process. When the designer is at the concept development stage, design studies can be employed to guide concept selection and to provide a record regarding why a particular concept was pursued. A design study in this context is the application of modeling and analysis to provide quantities useful to guiding concept selection. An example is the use of a computer model to simulate the effectiveness of different methods of aerodynamic controls, or the application of basic statics in evaluation of monocoque vs. framed chassis. Clear performance metrics, established before a design study is commenced, are required to ensure the study's output is useful. Specification of the scope of a design study is very important, as it is not effective if theoretical modeling and simulation require more resources than creation of experimental items. The author would like to suggest several design studies in particular.

1. Aerodynamic Control Layout

The current SUAVE prototype has been created with canard-type aerodynamic control surfaces for the reasons outlined earlier. This decision allowed the project to advance, so that more accurate weight and performance estimates are available for the current design. It is recommended to employ computer dynamics models such as those created within the NPS course ME4703 Missile GNC. Population of such models with Missile Lab output and

mass properties similar to those obtained from the current evolution of the SUAVE project will allow quantitative evaluation of the merits of several different control surface layouts. This will allow an early, high level review of the validity of modifications to the existing control surface layout.

2. Warhead Effectiveness

As mentioned earlier, the payload for the SUAVE has yet to be determined. This is therefore a critical area of development. Since small UAVs are an emerging threat category, it is expected that further development of this subsystem will require significant effort and resources. Definition of the scope of the research which should be expended on this question is extremely important, as vulnerability studies of a given system to a specific weapon's effects can individually require multiple live-fire experiments, which is likely beyond the scope of NPS thesis activities. The recommended ultimate goal of such studies is to determine what size of rocket is most appropriate from a cost standpoint; from a logistics standpoint; and from an "impact on the employment force" standpoint (i.e., how much additional workload is incurred from incorporating the SUAVE into an existing force structure).

LIST OF REFERENCES

[1] "Beyond Moore's law," *The Economist,* May 26, 2015. [Online]. Available: https://www.economist.com/news/science-and-technology/21652051-even-after-moores-law-ends-chip-costs-could-still-halve-every-few-years-beyond

[2] H. Mujtaba, "Intel Kaby Lake and Skylake processors get massive price cuts by retailers prior to AMD Ryzen launch – Core i7 7700K up for $299, Core i5 7600K for $199, Core i5 6600K for $179," wccftech, Feb 25, 2017. [Online]. Available: https://wccftech.com/intel-amd-price-war-ryzen-processors/

[3] L. V. Pham, "UAV swarm attack: protection system alternatives for Destroyers," Capstone project report, Dept. of Sys. Eng., NPS, Monterey, CA, USA, 2012. [Online]. Available: https://calhoun.nps.edu/bitstream/handle/10945/28669/12Dec_SE_Cohort_311-1120_Team_Crane.pdf?sequence=1&isAllowed=y

[4] D. Hawkins, "A U.S. 'ally' fired a $3 million Patriot missile at a $200 drone. Spoiler: The missile won." *The Washington Post*, March 17, 2017. [Online]. Available: https://www.washingtonpost.com/news/morning-mix/wp/2017/03/17/a-u-s-ally-fired-a-3-million-patriot-missile-at-a-200-drone-spoiler-the-missile-won/?utm_term=.9692c4aff4a9

[5] L. Dearden, "Revealed: ISIS developing weaponised drones in secretive programme," *Independent*, 20 October 2016. [Online]. Available: http://www.independent.co.uk/news/world/middle-east/isis-weapons-drones-uav-programme-development-weaponised-explosives-surveillance-terrorist-groups-a7371491.html

[6] J. Hsu, "Small weaponized drones become reality," *Discover Magazine*, Oct 31, 2016. [Online]. Available: http://blogs.discovermagazine.com/lovesick-cyborg/2016/10/31/small-weaponized-drones-become-battlefield-reality/#.WfoUEFtSzmE

[7] J. Binnie, "Iraqi forces use weaponised commercial drones," *IHS Jane's Defence Weekly*, 16 March 2017. [Online]. Available: http://www.janes.com/article/68779/iraqi-forces-use-weaponised-commercial-drones

[8] C. Dillow, "All of these countries now have armed drones," *Fortune*, Feb 12, 2016. [Online]. Available: http://fortune.com/2016/02/12/these-countries-have-armed-drones/

[9] "Wanted: Ideas for protecting against small unmanned air systems," DARPA, Aug. 11, 2016. [Online]. Available: https://www.darpa.mil/news-events/2016-08-11

[10] "Aerial Jenga," Flite Test, March 17, 2016. [Online]. Available: https://www.flitetest.com/articles/aerial-jenga

[11] K. Jones, interview, May 2016.

[12] K. Almanzan, "Naval Postgraduate School takes a lead in swarm drones," *90.3 KAZU NPR*, Jul 22, 2016. [Online]. Available: http://kazu.org/post/naval-postgraduate-school-takes-lead-swarm-drones

[13] F. Gady, "India to buy 245 U.S. Stinger air-to-air missiles," *The Diplomat*, April 01, 2016. [Online]. Available: https://thediplomat.com/2016/04/india-to-buy-245-us-stinger-air-to-air-missiles/

[14] D. Pugliese, "An American ally used a $3M Patriot missile to destroy a drone 'that cost 200 bucks,' U.S. general reveals," *National Post*, March 16, 2017. [Online]. Available: http://nationalpost.com/news/world/an-american-ally-used-a-3m-patriot-missile-to-destroy-a-drone-that-cost-200-bucks-u-s-general-reveals

[15] "Unmanned combat aerial vehicle," *Wikipedia*. Accessed Nov. 2, 2017. [Online]. Available: https://en.wikipedia.org/wiki/Unmanned_combat_aerial_vehicle

[16] J. P. Le Saint, "Innovation in the USAF," *Leading Edge*, June 16, 2015. [Online]. Available: https://leadingedgeairpower.com/2015/06/16/innovation-in-the-usaf/

[17] AeroVironment, "Switchblade," Mar. 21, 2017. [Online]. Available: https://www.avinc.com/images/uploads/product_docs/SB_Datasheet_2017_Web_rv1.1.pdf

[18] R. Smith, "AeroVironment will upgrade the Switchblade," *The Motley Fool*, May 11, 2016. [Online]. Available: https://www.fool.com/investing/general/2016/05/11/aerovironment-will-upgrade-the-switchblade.aspx

[19] Maj. Y. K. Qiu, Capt. K. Lobo, Capt. K. Grohe, "Survivability project low cost small tactical UAV," unpublished.

[20] "How to shoot down drones – MACHINE GUNS," YouTube, Apr 11, 2014. [Online]. Available: https://www.youtube.com/watch?v=rGLxKXtkHpY

[21] R. Ball, *The Fundamentals of Aircraft Combat Survivability: Analysis and Design, 2nd Edition*. Reston, VA, USA: AIAA Education Series, 2003.

[22] Python, M. (n.d.), “How not to be seen,” Youtube, posted Aug 31, 2015. [Online]. Available: https://www.youtube.com/watch?v=dTQYEkIvN2M

[23] Hobby King, *H-King Bixler 2 EPO 1500mm Ready to Fly*, 2017. [Online]. Available: https://hobbyking.com/en_us/hobbykingr-tm-bixlerr-tm-2-epo-1500mm-ready-to-fly-w-optional-flaps-mode-2-rt.html

[24] “Shot (pellet),” *Wikipedia*. Accessed Nov. 2, 2017. [Online]. Available: https://en.wikipedia.org/wiki/Shot_(pellet)

[25] M. Pearl, “We asked a military expert how scared we should be of an EMP attack,” *Vice*, May 7, 2015. [Online]. Available: https://www.vice.com/en_us/article/kwxq4v/we-asked-a-military-expert-how-scared-the-us-should-be-of-an-emp-attack-508

[26] J. Hooper, “Weapons physics,” unpublished.

[27] M. Driels, *Weaponeering: Conventional Weapon System Effectiveness, 2nd Edition*. Reston, VA, USA: AIAA Education Series, 2013.

[28] N.R. Jenzen-Jones, “US CBU-97/CBU-105 ‘sensor fuzed weapon’ cluster munition,” *Armament Research Services*, August 5, 2017. [Online]. Available: http://armamentresearch.com/us-cbu-97cbu-105-sensor-fuzed-weapon-cluster-munition/

[29] DroneShield, *DroneSentinel*, 2017. [Online]. Available: https://www.droneshield.com/sentinel

[30] “Phalanx CIWS,” *Wikipedia*. Accessed Nov. 2, 2017. [Online]. Available: https://en.wikipedia.org/wiki/Phalanx_CIWS

[31] M. Salita, *Memoirs of a Rocket Scientist: From Apollo to Space Shuttle to Minuteman to UAV/BPI, 1st Edition*. USA: CreateSpace Independent Publishing Platform, 2017.

[32] E. Fleeman, *Missile Design and System Engineering*. Reston, VA, USA: AIAA Education Series, 2013.

[33] K. Ulrich, S. Eppinger, *Product Design and Development*. New York City, NY, USA: McGraw-Hill Education, 2011.

[34] *Missile DATCOM User’s Manual – 2011 Revision*, AFRL-RB-WP-TR-2011-3071 Air Force Research Laboratory, Wright-Patterson Air Force Base, OH, USA, 2011.

[35] “HD supersonic P-800 Yakhont cruise missile launch,” Youtube, Aug 17, 2012. [Online]. Available: https://www.youtube.com/watch?v=4AW1XHUcAsQ

[36] “Speed of sound table chart,” Engineers Edge, Accessed Nov 9, 2017. [Online]. Available: https://www.engineersedge.com/physics/speed_of_sound_13241.htm

[37] “Centripetal force,” *Wikipedia*. Accessed Nov. 9, 2017. [Online]. Available: https://en.wikipedia.org/wiki/Centripetal_force

[38] “Circular motion,” *Wikipedia*. Accessed Nov. 9, 2017. [Online]. Available: https://en.wikipedia.org/wiki/Circular_motion

[39] A. Capaccio, “F-35 program costs jump to $406.5 billion in latest estimate,” *Bloomberg*, June 10, 2017. [Online]. Available: https://www.bloomberg.com/news/articles/2017-07-10/f-35-program-costs-jump-to-406-billion-in-new-pentagon-estimate

[40] P. Barrett, “The F-35 costs even more when you fly it,” *Bloomberg*, July 11, 2017. [Online]. Available: https://www.bloomberg.com/news/articles/2017-07-11/the-f-35-costs-even-more-when-you-fly-it

[41] C. Pierce, “The F-35 remains a nonfunctional, money-sucking nightmare,” *Esquire*, June 10, 2017. [Online]. Available: http://www.esquire.com/news-politics/politics/a13085304/f-35-oxygen-pilot/

[42] V. Insinna, “Pentagon kicks off intensive F-35 cost review,” *Defense News*, Oct 24, 2017. [Online]. Available: https://www.defensenews.com/air/2017/10/24/pentagon-kicks-off-intensive-f-35-cost-review/

[43] K. Mizokami, “This chart explains how crazy-expensive fighter jets have gotten,” *Popular Mechanics*, Mar 14, 2017. [Online]. Available: http://www.popularmechanics.com/military/weapons/news/a25678/the-cost-of-new-fighters-keeps-going-up-up-up/

[44] C. Skira, “Reducing military aircraft engine development cost through modeling and simulation,” Defense Technical Information Center, Wright-Patterson Air Force Base, OH, USA. Accessed Nov. 9, 2017. [Online]. Available: http://www.dtic.mil/dtic/tr/fulltext/u2/p014146.pdf

[45] M. Schnabel, “ME4704 Canard Development and Aerodynamic Analysis,” unpublished.

[46] I. Abbott, A. von Doenhoff, L. Stivers, “NACA report No. 824 summary of airfoil data,” Langley Field, Va., USA, 1945. [Online]. Available: https://ntrs.nasa.gov/archive/nasa/casi.ntrs.nasa.gov/19930090976.pdf

[47] Christopher Lovelace, Jon Silverberg, Paul Wright, Collier Crouch, Amy Gabriel, Tan, Choon Ming, Martin, Teo Huifen, Serene, Yang, Kangjie, Roy, “ME4704 missile design,” unpublished.

[48] Futaba, *S.Bus Servos*, 2017. [Online]. Available: https://www.futabarc.com/servos/sbus.html

[49] American Roller Bearing Company, *FRICTION & FREQUENCY FACTORS*, 2017. [Online]. Available: http://www.amroll.com/friction-frequency-factors.html

[50] H. Teo, “Aerodynamic predictions, comparisons, and validations using MissileLab and Missile DATCOM (97),” M.S. thesis, Dept. of Sys. Eng., NPS, Monterey, CA, USA, 2008. [Online]. Available: file:///C:/Users/Overlord_2.overlord-PC/Downloads/ADA494432.pdf

[51] Public Missiles Ltd, *G-10 Fins*, 2017. [Online]. Available: https://publicmissiles.com/secure/ComponentsFins.asp

[52] G. Verhaagen. “Effects of Reynolds Number on flow over 76/40-degree double-delta wings,” *Journal of Aircraft*, vol. 39, no. 6, pp. 1045–1052, 2002.

[53] “Aircraft stability,” CFI Notebook.net, Accessed Nov 28, 2017. [Online]. Available: http://www.cfinotebook.net/notebook/aerodynamics-and-performance/aircraft-stability

[54] Cesaroni Technology, *Pro-X*, 2017. [Online]. Available: http://www.pro38.com/

[55] “Parachute bay pressure vents,” Dave’s Hobby Page, Accessed Nov 28, 2017. [Online]. Available: http://home.earthlink.net/~david.schultz/rnd/pressurelag/parachute.html

[56] Giant Leap Rocketry, *Components Recovery*, 2017. [Online]. Available: https://giantleaprocketry.com/products/components_recovery.aspx

[57] Apogee Components, *CD3 HPR Kit (12G, 16G, 25G, 38G)*, 2017. [Online]. Available: https://www.apogeerockets.com/Ejection-Systems/CO2-Ejection-Systems/CD3-HPR-Kit-12g-16g-25g-38g

[58] PerfectFlite, *StratoLoggerCF Altimeter*, 2017. [Online]. Available: http://www.perfectflite.com/index.html

[59] Missile Works, *WRC+ Wireless Remote Control System*, 2017. [Online]. Available: https://www.missileworks.com/wrc/

[60] PerfectFlite, *StratoLoggerCF Users Manual*, 2017. [Online]. Available: https://www.apogeerockets.com/downloads/PDFs/StratoLoggerCF_manual.pdf

[61] “Drogue parachute,” *Wikipedia*. Accessed Nov. 29, 2017. [Online]. Available: https://en.wikipedia.org/wiki/Drogue_parachute

[62] FXC Corporation, *Releases - Cargo Parachute*, 2017. [Online]. Available: http://www.fxcguardian.com/products/aerial-delivery-cargo/releases-cargo-parachute

[63] FXC Corporation, *Releases - Cargo Parachute*, 2017. [Online]. Available: http://www.fxcguardian.com/assets/data_sheets/FXC15_Cargo_Release01.pdf

[64] D. Ang, M. Chin, L. Ozeck, B. Yee, M. Shelton, L. Tan, “ME4704 missile design project report,” unpublished.

[65] Public Missiles Ltd, *Airframes*, 2017. [Online]. Available: https://publicmissiles.com/product/airframes

[66] Arduino, *Getting started with the Arduino Due*, 2017. [Online]. Available: https://www.arduino.cc/en/Guide/ArduinoDue

[67] Arduino, *Sketches, Libraries and Tutorials*, 2017. [Online]. Available: https://playground.arduino.cc/Main/GeneralCodeLibrary

[68] Bosch Sensortec, *BNO055 Intelligent 9-axis absolute orientation sensor*, 2014. [Online]. Available: https://cdn-shop.adafruit.com/datasheets/BST_BNO055_DS000_12.pdf

[69] V. Dobrokhodov, interview, 3 Oct 2017.

[70] ODROID, *ODROID-C2*, 2017. [Online]. Available: http://www.hardkernel.com/main/products/prdt_info.php?g_code=G145457216438

[71] “Single-board computer,” *Wikipedia*. Accessed Nov. 29, 2017. [Online]. Available: https://en.wikipedia.org/wiki/Single-board_computer

[72] ROS, *ROS*, 2017. [Online]. Available: http://www.ros.org/

[73] ODROID, *ODROID-C2*, 2017. [Online]. Available: http://www.hardkernel.com/main/products/prdt_info.php?g_code=G145457216438

[74] Amazon, *DROK DC-DC Buck Boost Converter 5V-25V to 0.5-25V 2A High Efficiency Voltage Regulator 5V 12V Variable Volt Power Supply Stabilizers with Green LED Voltmeter for Car Battery Fan*, 2017. [Online]. Available: https://www.amazon.com/DROK-Converter-Efficiency-Regulator-Stabilizers/dp/B00GZHEPW6

[75] "Buck–boost converter," *Wikipedia*. Accessed Nov. 29, 2017. [Online]. Available: https://en.wikipedia.org/wiki/Buck%E2%80%93boost_converter

[76] LORD MicroStrain, *3DM-GX4 -25™ Attitude Heading And Reference System*, 2017. [Online]. Available: http://www.microstrain.com/inertial/3dm-gx4-25

[77] Raspberry Pi, *Raspberry Pi 3 Model B*, 2017. [Online]. Available: https://www.raspberrypi.org/products/raspberry-pi-3-model-b/

[78] "ABET definition of design," University of Nevada, Las Vegas. [Online]. Available: http://www.me.unlv.edu/Undergraduate/coursenotes/meg497/ABETdefinition.htm

THIS PAGE INTENTIONALLY LEFT BLANK

INITIAL DISTRIBUTION LIST

1. Defense Technical Information Center
   Ft. Belvoir, Virginia

2. Dudley Knox Library
   Naval Postgraduate School
   Monterey, California